Experimental studies on mouse slow and fast twitch muscles

by

Filli Nurhussen

November 2006
Technical Reports from
Royal Institute of Technology
Department of Mechanics
SE-100 44 Stockholm, Sweden

Abstract

This thesis deals with physiological and mechanical properties of fast and slow twitch mouse muscles. It discusses isometric, concentric and eccentric contractions of mouse *extensor digitorum longus* ('EDL') and *soleus* ('SOL') muscles. This project primarily investigated the behaviors of muscles, to give better understanding and improved descriptions for the human system, when subjected to impact or sustained high loading conditions.

Muscle force has been shown to be length and activation dependent. The effect of passive or active length changes on muscle force production was studied. Isometric activation showed a maximal force at optimum length for each individual muscle, to which all experiments were related. This optimum length was stimulation frequency dependent and maximum produced force shifted towards shorter length with increasing frequency.

Active shortening of maximally stimulated muscle was shown to produce reduced force, but also a reduced isometric force (force depression) following shortening, regardless of the shortening conditions and the method of muscle stimulation.

Steady state force depression (ΔF_{stdep}) was correlated with the instant force depression (ΔF_{idep}), pre-activation time, $t_0 - t_1$ and the work (W_S), performed by the muscle during shortening. It was positively correlated with the ΔF_{idep} when the shortening magnitude was varied ('VSM'). But in varying the shortening velocity ('VST'), it was negatively correlated with the instant force depression.

In active stretch, force was analogously enhanced during stretch, and this effect remained after stretch. Steady state force enhancement (ΔF_{stenh}) following muscle stretch was correlated with the instant force enhancement, (ΔF_{ienh}), pre-activation time, $t_0 - t_1$ and the work, (W_L), done on the muscle during stretch. It was positively correlated with ΔF_{ienh} when the stretch magnitude was varied ('VLM'). But in varying the stretch velocity ('VLT'), ΔF_{stenh} was negatively correlated with ΔF_{ienh}.

Furthermore, the rise time constant, (τ_r) of redeveloped isometric forces following the shortening and the fall time constant, (τ_f) of the relaxed isometric force following muscle stretch were calculated. In VSM, τ_r and F_{stdep} were positively correlated with each other, while in VST, they were negatively correlated. τ_f and F_{stenh} were negatively correlated in both VLM and VLT.

Preface

The work presented in this thesis was carried out at the Department of Mechanics at the Royal Institute of Technology (KTH) and Department of Physiology and Pharmacology at Karolinska Institute (KI) between June 2003 and November 2006.

First, I would like to thank Prof. Håkan Westerblad for giving me the opportunity to carry out the experiments at his laboratory and for his theoretical and experimental guidance together with Prof. Jan Lännergren. The time spent at the physiology lab in Karolinska Institute would be less enjoyable without them and their associates. I wish to thank Jin for her excellent work in preparing the specimen.

A special thank goes to my supervisor Prof. Anders Eriksson for his guidance and for his fruitful discussions with me.

I thank all my friends in the department of mechanics specially those on the 8'th floor for creating a great working atmosphere.

Last but definitely not least: Lilian, Diana, and Ing-Marie, I love you all.

Financial support from Swedish Research Council (VR) is gratefully acknowledged.

Stockholm November 2006

Filli Nurhussen

Symbols and abbreviations

Symbol	Description
a	Normalized activation level
F	Current force of muscle
F_{asymp}	Asymptotic force of muscle with time
F_{li}	Muscle force at initial length in experiment
F_{max}	Maximum muscle force at specific condition
F_0	Maximum isometric force of muscle, occurs at l_{op}
ΔF_{idep}	Instant force depression
ΔF_{stdep}	Steady − state force depression
ΔF_{ienh}	Instant force enhancement
ΔF_{stenh}	Steady − state force enhancement
f_{s}	Stimulation frequency in experiment
f_{t}	Tetanic stimulation frequency
$f_{0.5}$	Stimulation frequency for half the maximum tetanic force
l_{f}	Muscle fiber length
l_{i}	Initial muscle length in experiemnt
l_{op}	Optimum length of individual muscle
$l_{\text{op}}^{\text{av}}$	Group average optimum length
l_{r}	Magnitude of length change
l_{ss}	Sudden step length
$\dot{l}$	Time differential of muscle length
t_0	Time before length change is introduced
t_1	Time before stimulation starts
t_{r}	Shortening duration
t_{s}	Stimulation duration
W_L	Physical work done on muscle during lengthening
$W_{L,\text{max}}$	Maximum physical work done on muscle during lengthening
W_S	Physical work of muscle during shortening
τ_0	Rise time constant for initial activation at optimum length
τ_{f}	Fall time constant of relaxed isometric force
τ_{li}	Rise time constant for activation at initial length
τ_{r}	Rise time constant of redeveloped isometric force
σ	Stress defined as force per nominal area

Abbreviation	Description
ADP	Adenosine − tri − phosphate
AP	Action potential
ATP	Adenosine − di − phosphate
CE	Contractile element of muscle
EDL	Extensor digitorum longus
PCSA	Physiological cross sectional area
PEE	Parallel elastic element
SEE	Series elastic element
SOL	Soleus
SR	Sarcoplasmic reticulum
SS	Sudden step
T − tubules	Transverse tubules
VLM	Eccentric with varying lengthening magnitude
VLT	Eccentric with varying lengthening time
VSM	Concentric with varying shortening magnitude
VST	Concentric with varying shortening time

Contents

Chapter 1

Introduction

Skeletal muscle is a biological motor and is a highly organised tissue. Its main function is to actively generate force and produce movement through a process of contraction. It constitutes almost 50% of the body weight and consumes almost 50% of the body's metabolism, (Chaffin and Andersson 1991). Muscles are attached to bone by tendons, and cross one or several joints. They are under the direct control of the *voluntary* nervous system, sometimes referred to as the *somatic nervous system*, (Chaffin and Andersson 1991). Although many research works on muscle and its contraction properties have been done for centuries, some aspects of muscular force production have still not been resolved. For example, the exact mechanism of cross-bridge attachment and movement that are believed to cause relative movement of the myofilaments, and so produce force, are not clearly understood, (Nigg and Herzog 1999).

The main function of muscle is to produce mechanical energy during excercises such as swimming, cycling or accelerating at the start of a sprint. In such activities, muscles perform only positive work, which is lost by external friction, or increase the average potential or kinetic energy. Another important function of muscle is the ability to absorb mechanical energy during active stretch, (Cavagna et al. 1985; James et al. 1996).

The response of muscle to stimulus is determined by its fiber compostions. Generally, fibers are classified according to the duration of the twitch. Type I or slow-twitch fibers twitch with low maximum force and with long rise time to the maximum force and they are fatigue resistant. Example of such fiber is *soleus* ('SOL') muscle fiber. Type II or fast-twitch fibers have large maximum force and short rise time to maximum force. They are adapted to short duration and are therefore fast fatiguable. *extensor digitorum longus* ('EDL') muscle fiber is a good example of fast-twitch fiber, (Chaffin and Andersson 1991; Nigg and Herzog 1999).

Muscle length, velocity and activation are generally the most important parameters which affect muscle force production. At the optimum length a fully activated muscle produces maximum isometric force. After changing the muscle length passively from plateau region towards longer or shorter length, the muscle produces less isometric force than at its optimum length, (Nigg and Herzog 1999; Winters and Crago 2000).

The velocity dependence of muscle force is described in two aspects. In muscle active shortening or concentric contraction Hill model is being widely used. To use the Hill model in circumstances where the muscle is not fully activated, it is necessay to have some input to the model representing activation, (Allinger et al. 1996). In muscle lengthening or eccentric contraction different models have been proposed. Today, force depression following muscle shortening and force enhancement following muscle stretch are well-recognised and well-accepted properties associated with muscle contraction, however, the mecahnisms of these phenomena are weakly understood and are the focus of intense scientific debate (van den Bogert et al. 1998).

Many studies have been performed on the force depression following muscle shortening and force enhancement following muscle stretch. Although there is no accepted scientific paradigm for force depression following muscle shortening and force enhancement following stretch, the sarcomere length non-uniformity theory has received more support than any other competing theory. However, the mechanism underlying these properties is not well known, (Edman et al. 1993; Herzog and Leonard 1997; Maréchal and Plaghki 1979). Fredrick (2004); Chaffin and Andersson (1991) speculated more than two decades ago that force enhancement may be associated with the recruitment of an elastic component which is arranged in parallel to the contractile element. They speculated that this parallel elastic component was able to be recruited upon active stretch.

1.1 Anatomy and physiology

Architecture of skeletal muscles

Muscles attach at the origin (proximal end) and insertion (distal end) points. Both sides end in tendons that attach to bone. The geometrical arrangement of the fibers and connective tissue plays an important role in determining muscle force and mechanical behavior, (Chaffin and Andersson 1991; Winters and Crago 2000). Tendons vary considerably in shape, ranging from flat bands to cylindrical cords. They may be short and thick or long and thin. The shape of the tendon affects its physical properties and also determines how the muscle fibers can be geometrically arranged. Muscle fibers generally attach to aponeurosis or tendon in parallel arrays, (Nigg and Herzog 1999), Fig. 1.1.

Surfaces of attachment are increased by the attachment of muscle fibers along the sides of tendon and aponeurosis. In almost all cases, the muscle fibers attach at a slight angle with respect to the line of pull of the tendon, called the *pennation* angle, (Winter 2005).

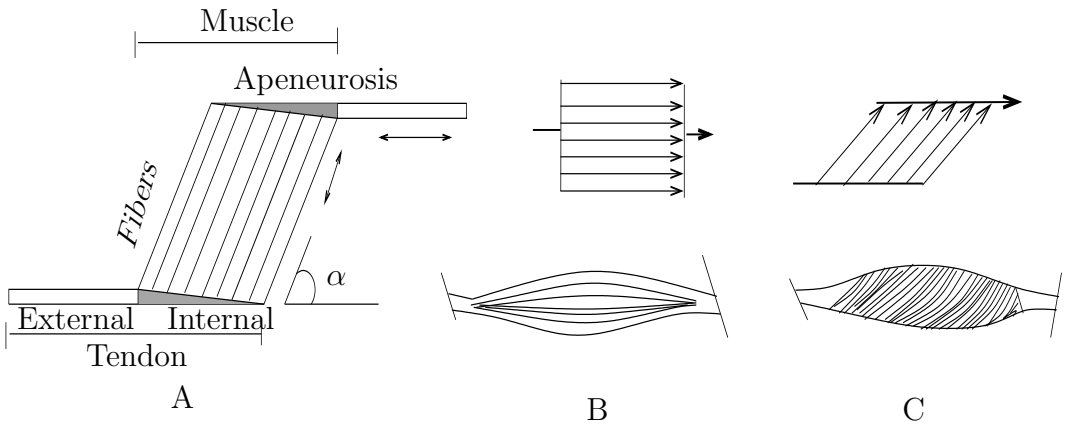

Figure 1.1: Relation among muscle fibers and tendons in pennated muscle. Muscle fibers lie in parallel, have the same length, and are oriented at the same angle α to the tendon axis of pull (A). (B) and (C) are examples of pennated muscles and corresponding force directions. A is re-drawn from Nigg and Herzog (1999)

Pennation angle increases as the length of the muscle-tendon unit is shortened by rotation of the joint. In an active length change of a muscle, there can be even greater variations in pennation angle. In SOL muscle for example, pennation angles can be as large as 50° when it is contracting maximally at short lengths (e.g. 90° knee angle, 140° ankle angle), (Lieber and Fridén 2000).

The structure of muscles

Muscle consists of muscle cells, also termed muscle fibers, connective tissues, and nerve elements. Cells consist of subunits called *myofibrils*, which are the true contractile elements. The contractile unit in the myofibril is called the *sarcomere*. The myofibrils, in turn, consist of two types of filamentous subunits which are overlapping. These two subunits within the myofibril are the thick myofilament consisting mostly of the protein *myosin*, and the thin ones containing *actin*, Fig. 1.2. The different bands of a muscle fiber are illustrated in Fig. 1.2.

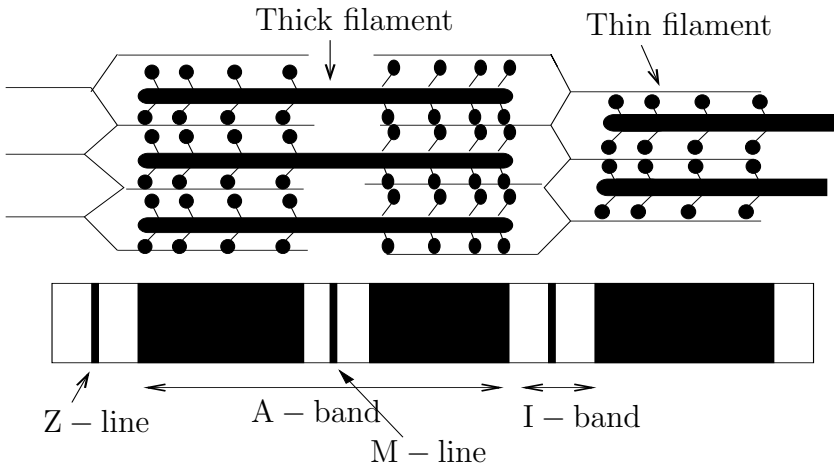

Figure 1.2: Schematic illustration of the basic structure of contractile unit of the muscle, the sarcomere. Thick horizontal lines represent myosin filaments, thin horozontal lines are actin filaments, and cross-hatched lines with round edges are cross-bridges. Re-drawn from Rassier et al. (1999) and modified.

The dark bands are called A-bands and consist of overlapping thick and thin filaments (myosin and actin). The light band, or I-bands, consist of of thin filaments (actin) only. Through the center of the A-band there is a narrow lighter band, the H-band, and transecting this band is the M-line. The I-band also has a central dense transverse band, the Z-line, (Chaffin and Andersson 1991; Nigg and Herzog 1999; Winter 2005).

Muscle fiber types

Within the slow- and fast-twitch categories, scientists have identified three main fiber types in human muscle: Type I, Type IIa and Type IIb. Type I is slow-twitch fiber, while types IIa and IIb are fast-twitch fibers.

Type I fibers are called slow-twitch because their maximum shortening velocity $V_{\max}$ is lower than that for fast twitch fibers. Also referred to as 'slow oxidative' fibers, Type I fibers have a high *aerobic* capacity. Aerobic metabolism is a more efficient energy pathway than *anaerobic* metabolism, providing much more energy per unit of fuel and allowing the use of multiple types of fuel (glucose, fats and lactate). As a result, Type I fibers are more efficient than Type II ones. Type I fibers do not produce forces as great nor as quickly as the fast-twitch types, but they are very fatigue-resistant, (Fredrick 2004; Chaffin and Andersson 1991). This type of muscle fibers is dominant in SOL muscles, located for example in human leg. It is situated deep to *gastrocnemius*, being a broad flat muscle wider in its middle section and narrow below, (Palastanga et al. 2002).

Type II fibers, which are called fast-twitch muscle fibers, have the highest $V_{\max}$ and produce the greatest force, but also suffer the highest rate of fatigue. They have large

anaerobic capacities but little potential for aerobic fuelling. Their main fuel source is glycogen, and since glycolysis is a fast energy-delivery pathway, they can burn through glycogen stores quickly. Glycogen can not be replenished during exercise, and its depletion results in fatigue, (Fredrick 2004; Chaffin and Andersson 1991). This type of muscle fibers is almost exclusive in EDL muscles, found for example in human leg. It is situated at the lateral part of the front of the leg.

Sliding filament theory

According to the sliding filament theory, (King et al. 2004; Smith and Geeves 1995), myosin filaments grab on to actin filaments during a contraction by forming chemical bonds called cross-bridges. By the use of these cross-bridges, the thick filaments pull the actins toward the center. Because the actins are attached to the Z-line, this sliding movement shortens the length of the entire sarcomere. During a contraction, the filaments maintain their original length and only the I band actually gets compressed. In a muscle fiber, the signal for contraction is synchronized over the entire fiber so that all of the myofibrils that make up the sarcomere shorten simultaneously, (Nigg and Herzog 1999; Chaffin and Andersson 1991; Winters and Crago 2000; Gordon et al. 2000).

The relative length of each band depends on the state of contraction of the muscle. Since when contracting, the thick and thin filaments slide relative to each other, the A-band remains constant in length. The contractile unit in the myofibril, (sarcomere), is defined by the distance between two Z-lines, to which the I-bands are attached. The interaction and sliding of the filaments relative to each other is the basic mechanism of muscle contraction. This model of muscle contraction is called *the sliding filament model of muscle*, (Huxley 1974; Chaffin and Andersson 1991).

Physiological cross sectional area ($PCSA$)

Physiological cross sectional area ($PCSA$) is the ratio between the volume of muscle and muscle fiber length. It affects the maximum force output of skeletal muscle. A large physiological cross sectional area is a sign of having either more fibers or fibers with larger diameters. That means that the greater $PCSA$ the muscle has, the larger force it can produce, (Nigg and Herzog 1999). If two muscles have identical fiber lengths and pennation angles, but one muscle has larger diameter (more fibers and thus larger $PCSA$), they produce different maximum force. Although the force-length curves have the same basic shape, the force corresponding to the muscle with larger $PCSA$ is larger provided that their fiber-type distributions are identical and that they produce the same force per unit area, (Nigg and Herzog 1999; Chaffin and Andersson 1991). This shows that while structural properties affect the extrinsic muscle properties, they have no effect on its intrinsic properties, Fig. 1.3, (Lieber and Fridén 2000). $PCSA$ is defined as

$$PCSA = \frac{m \ \cos(\alpha)}{\rho l_f} \tag{1.1}$$

where m is muscle mass, α is the pennation angle, ρ (1056 kg/m^3) is density of muscle, and l_f is fiber length. Other definitions have, however, been used. In the present work, with essentially parallelly organized muscles ($\cos(\alpha) \approx 1$) the $PCSA$ is defined as

$$PCSA = \frac{m}{\rho l_m} \tag{1.2}$$

where l_m is muscle length.

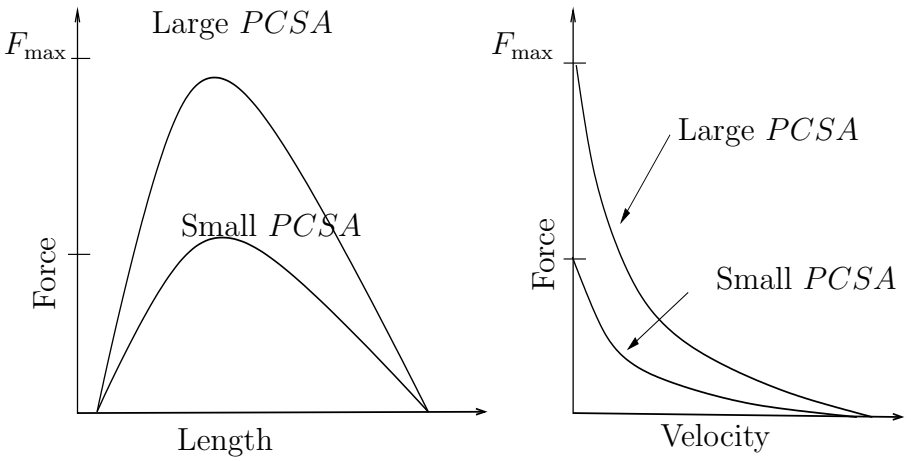

Figure 1.3: Schematic demonstration of two muscles with identical fiber lengths and pennation angles, but different physiological cross sectional areas ($PCSA$). Force-length relationship (left panel) and force-velocity relationship (right panel). Re-drawn from Lieber and Fridén (2000)

Fiber length

The force generated by muscle is also affected by the fiber length. If two muscles with identical $PCSA$ and pennation angles but with different fiber lengths, are compared, the peak absolute force of the force-length curves is identical, but the absolute muscle active range is different, Fig. 1.3. For the same reason that the fiber length increases the active muscle range of the force-length relationship, it causes an increase in the muscle's absolute maximum contraction velocity ($V_{\max}$). Again, while the fiber length increase causes an increase in these extrinsic properties, it has no effect on the intrinsic properties of the muscle, Fig. 1.4. Some muscles, like human *sartorius* muscle, are slender and contain long fibers in series with short tendons. The sartorius muscle is a long thin muscle that runs down the length of the thigh. It is the longest muscle in the human body. The fibers of this muscle are oriented parallel to the line of pull of muscle. Muscles like sartorius muscle generate low forces. However, due to the length of their fibers they exert force over a large length range. Other muscles like *gastrocnemius* muscle, have many short fibers in parallel that make a considerable angle with the line of pull of the muscle. It is a powerful muscle that is in the back part of the lower leg (the calf) and runs from its two heads just above the knee to the heel, and is involved in standing

and walking. In the *gastrocnemius* muscle the fibers are attached to the long and compliant *Achilles tendon*. Muscles like the *gastrocnemius* muscle are particularly suitable for generating high forces, albeit over a small length range, (Lieber and Fridén 2000).

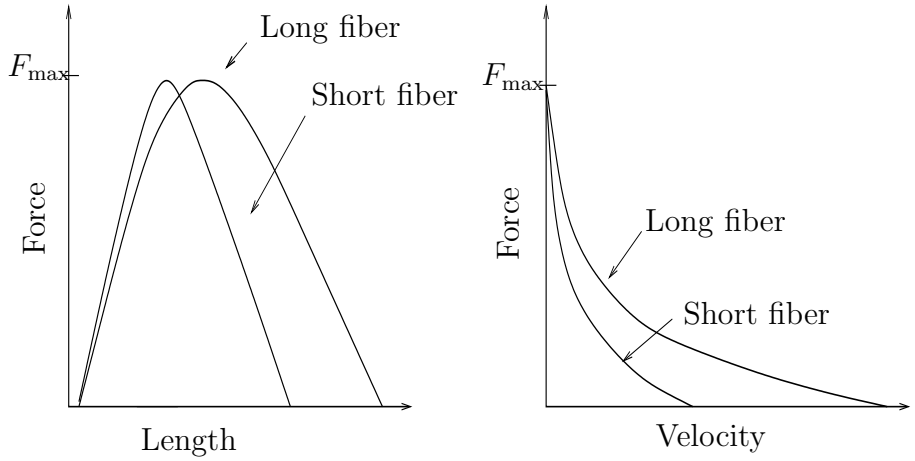

Figure 1.4: Schematic demonstration of the two muscles with identical PCSA and pennation angles but different fiber lengths. Force-length relationship (left panel) and force-velocity relationship (right panel). Re-drawn from Lieber and Fridén (2000).

Fiber arrangement within muscle

The effects of architecture on the contractile properties of muscle are described briefly as follows, (Lieber and Fridén 2000): Assume that you have two muscles with identical volume, filled with contractile elements (sarcomeres). Imagine that one of the muscles has larger cross sectional area than the other one and let the sarcomeres be arranged in series so that they form either long or short fibers, Fig. 1.5. Provided that all sarcomeres contract with the same amount, the muscle with longer fibers can exert force over a larger range of muscle length, but produces less force than the muscle with shorter fibers and larger $PCSA$. The two muscles produce the same amount of mechanical work because they consist the same number of sarcomeres, under the condition that each sarcomere is assumed to produce a given amount of work, (Nigg and Herzog 1999). Two good examples of such a difference are *sartorius* muscle which is slender and contains long fibers in series, and *gastrocnemius* which has many short fibers in parallel. .

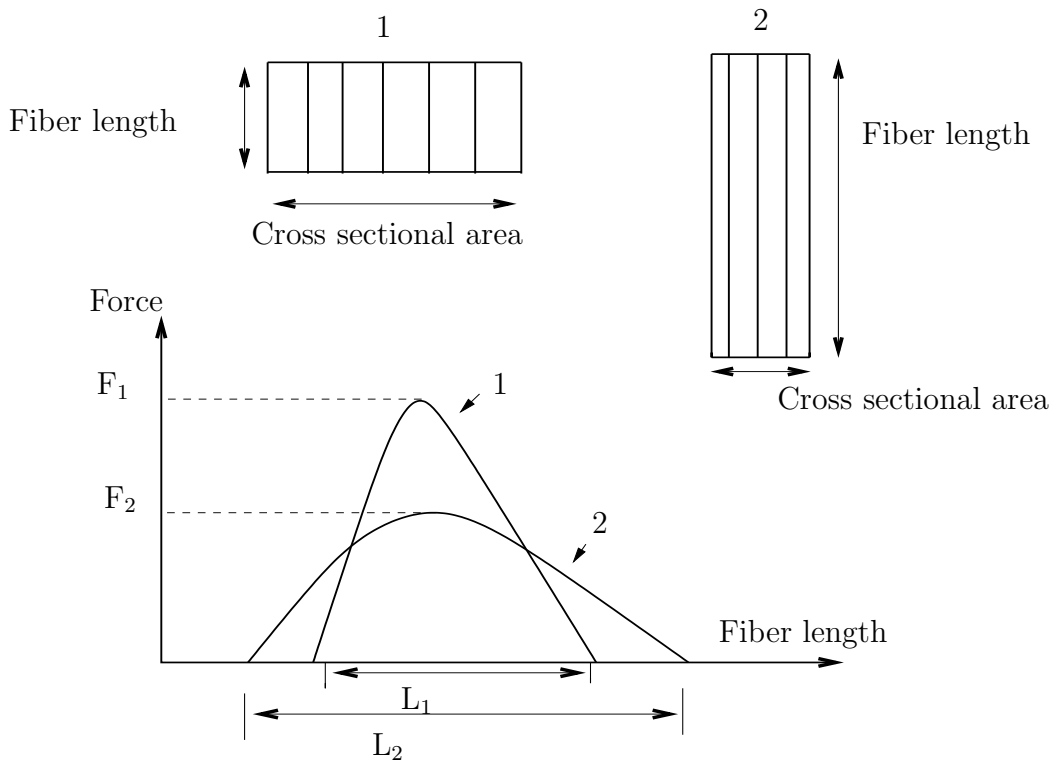

Figure 1.5: Schematic demonstration of force-length relationship of two muscles with different cross-sectional areas and fiber lengths, but equal volumes. Redrawn from Nigg and Herzog (1999)

1.2 The response of muscle stimulation

When a muscle is stimulated by a single pulse an action potential is elicited which causes the muscle to produce a twitch. The twitch has longer duration than the action potential, but duration varies considerably from muscle to muscle. The response of a whole muscle to a stimulus depends primarily on: the electrical strength and frequency of the stimulus; the fiber composition of the muscle; the length of the muscle; and the velocity of the muscle contraction, (Chaffin and Andersson 1991; McMahon 1984). As the electrical strength in a single stimulation pulse (Voltage) increases, additional fibers are recruited, until a maximum contraction occurs; thus, the amplitude of the twitch reaches its maximum. This is an indication that almost all fibers in the muscle are activated or recruited at a certain stimulation strength. (Chaffin and Andersson 1991; McMahon 1984). If a second electrical stimulus is delivered before the muscle response to the first is ended, a greater contraction force will occur. This phenomenon is known as frequency or temporal summation, and occurs even if the second stimulus is equal to the first, and if all motor units have contracted as a result of the first stimulus. When a series of impulses are delivered regularly at a rapid enough frequency, a sustained maximal contraction occurs, known as *tetanus*, (Chaffin and Andersson 1991; McMahon 1984), Fig. 1.6. The rate

at which stimuli must be applied to cause tetanus varies between muscles. In the present studies, it was shown that tetanic frequency (at 10 V stimulation voltage) was about 70 Hz in SOL and 100 Hz in EDL.

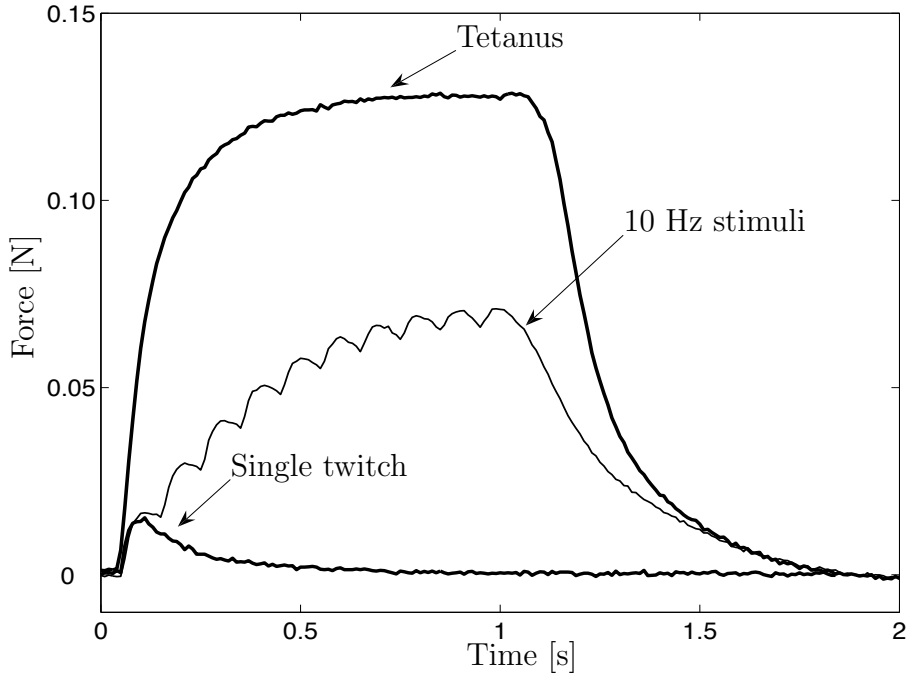

Figure 1.6: Example of twitch and tetanus of SOL muscle from the performed experiments. When a series of stimuli is given, muscle force rises to an uneven plateau which has a ripple at the frequency of stimulation. As the frequency is increased, the plateau rises and becomes smoother, reaching a limit as the tetanus becomes smooth.

1.3 Excitation-contraction coupling

The electrical impulse called *action potential* ('AP') initiates contraction. The AP propagates along the sarcolemma, membrane, of muscle fibers and spreads to the interior of fibers through the *transverse tubules* ('T-tubules'), invaginations of the cell membrane marked with T in Fig. 1.7. When the electrical signal reaches the T-tubules, Ca^{2+} is released from adjacent *sarcoplasmic reticulum* ('SR'). Contraction is initiated when Ca^{2+} binds with troponin. When a binding site on the actin filament becomes available, the myosin head binds to the active site and a cross-bridge is formed. By splitting of *Adenosine-tri-phosphate* ('ATP') into *Adenosine-di-phosphate* ('ADP') plus a *phosphate* ('P_i'), energy is provided to cause the cross-bridge head to move and so attempt to pull the thin filaments past the thick filaments. At the end of the cross-bridge movement, an ATP molecule is thought to attach to the myosin portion of the cross-bridge so that the cross-bridge can release from its attachment site, go back to its original configuration, and be ready for a new cycle of attachment, (King et al. 2004; Nigg and Herzog 1999; Gordon et al.

2000; Gissel and Clausen 2000), Fig. 1.7.

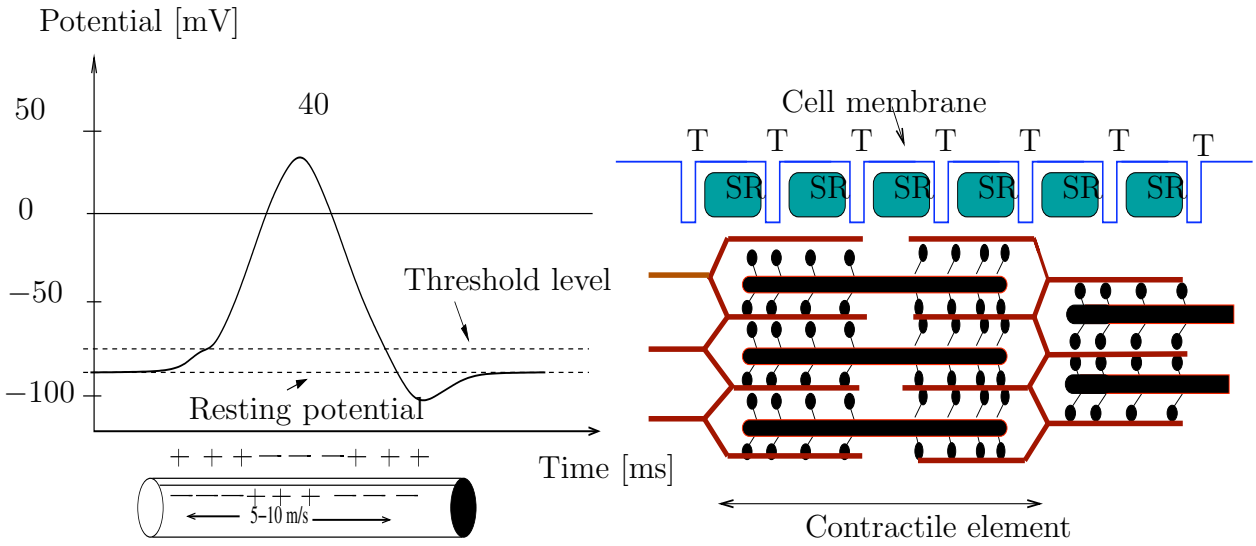

Figure 1.7: Left panel: Schematic illustraion of a single muscle fiber action potential (top) and the corresponding propagation of the action potential along the muscle fiber (bottom). Right panel: Schemetic illustration of T-tublues in a section of a muscle fiber and its association with the sarcoplasmic reticulum (SR) and the contractile myofilaments, (Nigg and Herzog 1999).

1.4 Mechanical aspects of muscle

The activation of a muscle (contraction) results in tension within the muscle. In the experiments reported below, the three cases of contractions are introduced in the following way:

1. *Isometric contraction* is one in which muscle length does not change during the contraction. In reality, no contraction is completely isometric because, on a fibril level, the distance between the Z-lines always shortens. The term describes contractions in which the external length of the muscle remains unchanged. Because the muscle does not grossly move, no work is done, 2. *Concentric contraction* is when a muscle shortens while activated and produces force which is less than the maximum isometric force at the same muscle lengths. Depending on the shortening velocity, which is related to muscle property and the compliance of the surrounding system, the reduction in force varies. 3. *Eccentric contraction* is when a muscle is stretched while activated and produces more force than the maximum isometric force at the corresponding muscle length.

1.5 Mechanical model of muscle

Many different mechanical models have been suggested for the description of muscle function. Many of these are consisting of rheological components. Such models, although very different in forms, are often referred to as Hill models, (Winters and Crago 2000; Winter 2005; McMahon 1984; Campbell and Lakie 1998; Ettema and Meijer 2000; Lagreneur et al. 1996). One example is shown in Fig. 1.8.

Three elements compose the mechanical model of the muscle influencing its mechanical behavior and effecting contraction: 1. The contractile element, ('CE'); 2. The series elastic element, ('SEE'); and 3. The parallel elastic element, ('PEE'), Fig. 1.8. The contractile element represents the myofibril, which are the active part of the muscle and are competent to produce tension. The parallel elastic element represents the connective tissue surrounding each muscle fiber, groups of fibers and the whole of the muscle. The series elastic element refers mainly to the tendons of the muscle which are placed in series with the contractile and parallel elastic elements. The activation of muscle results in tension within the muscle and this contraction can occur in a variety of ways, some of which are mentioned above, (Winter 2005; McMahon 1984).

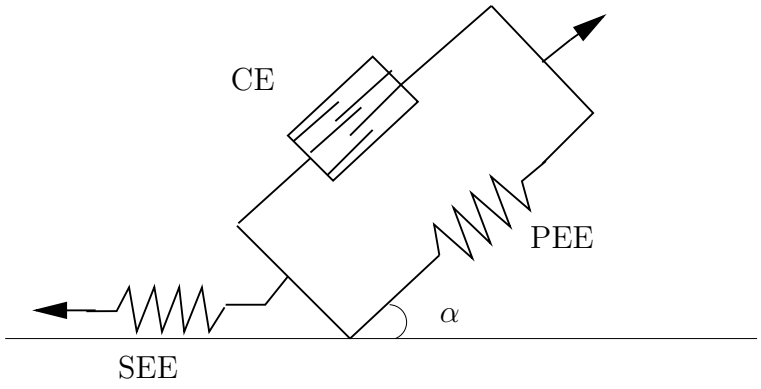

Figure 1.8: Example of Hill-type Muscle-tendon model which consists of a contractile element (CE), series elastic element (SEE), and parallel elastic element (PEE). α is the pennation angle, (Nigg and Herzog 1999; Campbell and Lakie 1998; Zajac 1989).

The objective of this experimental work has been to study and verify a generalized model for muscle force production, aiming at inclusion of the muscular model in a simulation for mammal, primarily human, movements and work. In order to be suited for the considered usage, the description should be the basic form

$$F(t) = F(l, \dot{l}, a; t) \tag{1.3}$$

where $F(t)$ is the muscular force at time t, l is the current muscle length, $\dot{l}$ is the current time differential of the legnth, and a is the normalized activation measure.

1.6 Outline of thesis

This thesis describes a set of experiments on mouse *extensor digitorum longus* ('EDL') and *soleus* ('SOL') muscles, aimed at finding numerical descriptions of their behaviors in isometric, concentric and eccentric contractions

Chapter 2 deals with basic experimental studies on muscle force-length and force-velocity relationships. Force-length curves corresponding to maximally and sub-maximally stimulated muscles are shown. Force-velocity relationships describing the shortening and stretch velocities are also shown. Isometric forces with different stimulating frequencies were measured and are shown in force-time curves. Emphasis is given to the pre-activation of muscle stimulation.

Chapter 3 deals with the effects of concentric contraction on force production in maximally stimulated EDL and SOL muscles. Force depression during and following muscle shortening, of different shortening magnitudes and velocities were studied. Some of the mechanisms behind this force depression are commented on.

Chapter 4 deals with the effect of eccentric contraction on force production in maximally stimulated EDL and SOL muscles. Force enhancment during and following muscle stretch were studied at different stretch magnitudes and stretch velocities. The mechanisms behind force enhancement following muscle stretch are commented on.

In chapter 5, some conclusions are given and several suggestions are forwarded for future directions of the work presented in this thesis.

1.7 Objectives

In this thesis, muscle force production, in different situations were studied. The aim was to determine and describe the depressant effect of active shortening and enhancing effect of active stretch of maximally stimulated skeletal muscle. It was also the objective of this study to investigate the mechanisms behind the force depression following muscle shortening and force enhancement following muscle stretch.

Chapter 2

Development of experimental paradigm

2.1 Introduction

In biomechanics, the primary interest in skeletal muscle modelling has been the representation of the forces of entire muscles. The primary approach for this type of skeletal muscle modelling has been to develop more or less complex numerical descriptions. These are commonly related to the basic model by Hill. The term Hill-type models are now used for diverse models, composed of rheological elements, such as springs and dashpots, arranged in series and/or in parallel, regardless of the relation to the basic model, (Allinger et al. 1996). This model contains elements that have force-velocity properties related to the speed of shortening and the corresponding maximal tetanic force obtained at optimum muscle length, (Zajac 1989). The behavior is complex, and most models have been developed to describe certain physiologically relevant aspects. Extrapolation of Hill-based muscle models to complex contractile conditions may be unreliable (van den Bogert et al. 1998). As an example, it is well-known that these models do not describe force-depression or force-enhancement correctly, and in particular the remaining effects after deactivation of muscles, following active shortening or stretch. The modelling has normally started from performed sets of physiological experiments, and are therefore seen in relation to these physiological aspects. For general simulation contexts, for instance in dynamical simulations of human movement, the models are more or less useful. As an example, much work has gone into the description of the static force production of muscles for isometric or isotonic situations. A typical result is the force-length relation for a muscle, showing that the activated force is maximum for an optimum length, corresponding to an optimum filament overlap in the sarcomere.

A dynamical simulation of movement, however, must be able to describe more or less arbitrary combinations of muscle lengths and lengthening velocities. In particular, muscles are capable of generating forces while lengthening or working eccentrically against a load. Indeed, there is a radically different shape to the force-velocity curve on the lengthening than on the shortening side, cf. Figs. 2.6, 2.7. A force enhance-

ment of considerable magnitude can thus be obtained for the eccentric contractions, (Allinger et al. 1996; Morgan et al. 2000):

Force-velocity relationship refers to force production from the muscle according to its length velocity. The tension decreases as it shortens (concentric contraction, negative velocity) while the reverse is true in lengthening (eccentric contraction, positive velocity), (Zajac 1989). During concentric contraction, the decrease of tension has been attributed to two main causes: (Bagni et al. 2002; Zajac 1989)

1. A major reason appears to be the loss in tension as the cross-bridges in the contractile element break and then reform in a shortened condition.
2. A second cause appears to be the fluid viscosity in both the contractile element and the connective tissue. Such viscosity requires internal force to overcome and therefore results in a lower tendon force (Zajac 1989).

Physiologically, the most important factor determining the force-velocity curve is the rate of the cross-bridge cycling process. The transition from attached to detached state requires ATP. Rate constants of the different transitions differ between slow-twitch and fast-twitch muscle fibers and depend on the velocity of filament sliding, and thereby determine the force produced. Although fibers can be distinguished on the basis of their metabolic properties, fatigue resistance, and mechanical responses, it is common just to distinguish between fast-twitch and slow-twitch muscles.

This chapter consists of the following parts. After a definition of the scope and objective of the present work, the setup of an experimental study of mouse *soleus* ('SOL') and *extensor digitorum longus* ('EDL') muscles is described in section 2.3. The results from this study, and some conclusions from the experiments with bearing on the numerical modelling are given in section 2.4.

2.2 Scope

The main objective of this study was to study methods for investigating the muscular force as function of activation, length and velocity, during and after muscular work. To bring out this point, we measured force variation with time for different tension-length variations and rates of stimulation.

With the planned numerical modelling as aim, a parameterized time evaluation for experiments was chosen according to Fig. 2.1. This parameterized experimental setup was chosen as it is closely related to a numerical simulation model in, e.g., finite element form. The key feature of this viewpoint is that the force in the muscle is described as a time-dependent function of an activation measure, but also as dependent on the instantaneous muscle length and the time differential of this length, being positive (stretch) or negative (shortening). Formally, this viewpoint is hypothesized by the expression:

$$F(t) = F(l, \dot{l}, a; t) \tag{2.1}$$

where $F(t)$ is the muscular force at time t, l is the current muscle length, $\dot{l}$ the current time differential of the length, and a a normalized activation measure, all parameters being functions of time t. This basic form does thereby not take the history into account, although this is known to be an important factor, and should be considered in further work.

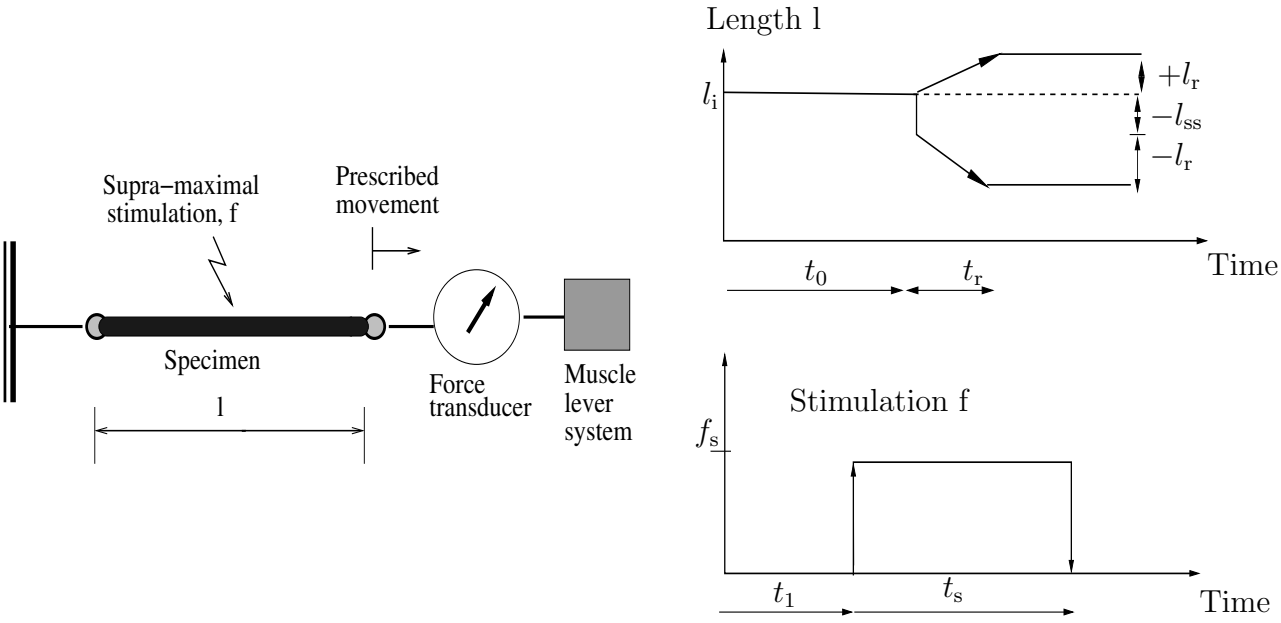

Figure 2.1: Schematic diagram of experimental apparatus and measurement methods. Force was measured as function of time, for prescribed variations in specimen length and muscle stimulation

Following most experimental and modelling papers, it is in the present work hypothesized, that all muscles behave in the same way, with only a scale factor F_0 as parameter; this is the maximum, fully activated isometric load level, at an optimum muscle length l_{op}. For the experiments below, all measured forces are thereby normalized with respect to this value for each individual muscle. Without consideration of history, this method of representation assumes that the force in a muscle can be seen according to

$$F = F_0 \cdot \psi(l, v, a) \tag{2.2}$$

with $v \equiv \dot{l}$, the length change velocity.

2.3 Experimentation

2.3.1 Animals

Adult male mice (NMRI strain) were housed at room temperature and fed ad libitum. The mass of the mice was about 30 g. Animals were killed by rapid neck dis-articulation. The procedure was approved by the Stockholm North local ethical committee.

2.3.2 Muscle preparation and solutions

EDL and SOL muscles were isolated. To allow for an evaluation of the physiological cross-sectional area ('$PCSA$'), the masses of the muscles were measured after the experiments. The nominal area was then evaluated from tissue density $\rho = 1056\,\mathrm{kg/m^3}$ and individual length. Small stainless steel loops were tied, using thin nylon thread, to the tendons very close ($\sim$ 0.1 mm) to the isolated muscle. The muscle was then mounted between a force transducer, Dual-Mode Muscle Lever System (Aurora Scientific, Ontario, Canada), in a lab-built stretch/shortening device, Fig. 2.1.

During the experiment, the muscle was bathed in continuously stirred Tyrode solution of the following composition (all in mM): 121 NaCl, 5 KCl, 0.5 $MgCl_2$, 1.8 $CaCl_2$, 0.4 NaH_2PO_4, 0.1 NaEDTA, 24 $NaHCO_3$, 5.5 glucose. Fetal calf serum (0.2%) was added to the solution. The solution was bubbled with 95%O_2 / 5%CO_2 (pH7.4). Experiments were performed at room temperature ($\sim 24°C$). Stimulation was started following at least 30 minutes of rest after the muscle was mounted in the muscle bath. The testing of each muscle specimen took about 4 hours.

2.3.3 Experimental apparatus and stimulation

The experimental setup allowed a prescribed length change to be applied to the muscle; the precision in a desired length variation was very high. It also allowed a prescribed stimulation with a certain frequency and voltage; the precision in these was very high. Isometric contractions were produced at 1 min intervals by trains of supra-maximal current pulses (10 V, 0.5 ms duration), which were applied via platinum plate electrodes placed on each side of the muscle, at specified frequencies. The stimulation train durations were 600 ms for EDL muscle and 1000 ms for SOL muscle. Passive forces were measured at the same lengths.

The length of each muscle was adjusted to allow maximum tetanic force to be generated. This was done through stretching the muscles by small steps and measuring the active mechanical force in every step; the length giving the highest force was noted as an optimum length l_{op} and was used as basis for the length variations in subsequent experiments. This force was denoted as F_0 and was seen as a preliminary optimal force. A final F_0 for each individual muscle was found later, cf. below.

All stimulation patterns and muscle puller length changes were controlled via computer, with the use of digital pulses and digital-to-analog outputs, respectively. The synchronization between stimulation and displacement was controlled by a lab-built digitimer.

2.3.4 Data recording

Records of stimulation, force and muscle length were stored in a computer. The sampling frequency was 333 Hz. Obtained results were maintained during experiments

Table 2.1: Basic data of EDL muscle individuals

Muscle	l_{op} [mm]	Mass[mg]	PCSA[mm^2]	F_0[N]	σ [kPa]
EDL − 1	9.50	14.10	1.41	0.33	233
EDL − 2	9.35	13.50	1.37	0.34	246
EDL − 3	9.60	14.20	1.40	0.34	240
EDL − 4	9.70	11.70	1.14	0.26	231
EDL − 5	9.55	11.20	1.11	0.24	220
EDL − 6	9.35	12.80	1.30	0.31	242
EDL − 7	9.85	14.80	1.42	0.38	265
Average	9.56	13.19	1.31	0.31	240
SD	0.18	1.35	0.13	0.05	14

and stored for further post-processing.

2.3.5 Testing paradigm

The testing sequence was reflective of the planned simulation process. The experimental method is schematically described in Fig. 2.1, where the right half describes the activation and displacement sequences, used to allow concentric, isometric and eccentric contractions at different stimulation frequencies, but also different timings of the activation in relation to the length variation. By choosing a suitable initial length, l_i, a velocity, l_r/t_r and a timing, described by $t_0 - t_1$, different combinations of length and velocity can be obtained and the corresponding force variations registered. The basic protocol was to apply a given length and stimulation pattern to muscle. After changing parameters, the procedure was repeated with at least 1 min interval. Isometric situations and iso-velocity ramps were studied in the same manner. In concentric contraction, the shortening was initiated at $l = l_i = l_{op} + l_r$ mm. In eccentric contraction the initial length was $l = l_i = l_{op} - l_r$ mm, in both cases ending at l_{op}.

2.4 Experimental results

First an optimum length, l_{op} was obtained for each individual muscle specimen. Corresponding isometric force is F_0. A nominal force $\sigma = F_0/PSCA$ was evaluated, Tables 2.1–2.2.

2.4.1 Twitch

Twitches for muscles of each type were studied. Twitch contractions were recorded at lengths: $l_{op}+2$ mm, $l_{op}+1$ mm, l_{op} and $l_{op}-1$ mm, for all individual muscles. The

Table 2.2: Basic data of SOL muscle individuals

Muscle	l_{op} [mm]	Mass[mg]	PCSA[mm^2]	F_0[N]	σ [kPa]
SOL − 1	9.20	10.60	1.09	0.13	121
SOL − 2	9.65	12.60	1.24	0.16	125
SOL − 3	9.33	10.80	1.10	0.13	118
SOL − 4	9.90	10.40	1.00	0.11	115
SOL − 5	9.50	9.40	0.94	0.12	127
SOL − 6	9.05	12.8	1.34	0.17	129
SOL − 7	9.35	9.60	0.97	0.11	112
Average	9.43	10.89	1.10	0.13	120
SD	0.29	1.34	0.15	0.02	7

shapes of these contractions differ in that the time course of the twitch contraction measured at $l_{op}+2$ mm was slower than that measured at $l_{op}-1$ mm. This behavior was observed in all muscles. Examples of a single twitch of EDL and SOL muscles are shown in Fig. 2.2. As shown in Tables 2.3–2.4, twitch kinetics were assessed by measuring the contraction time, i.e from the onset of force production until peak force was produced, and half relaxation time, i.e, from peak force production until force reduced to 50% of the peak.

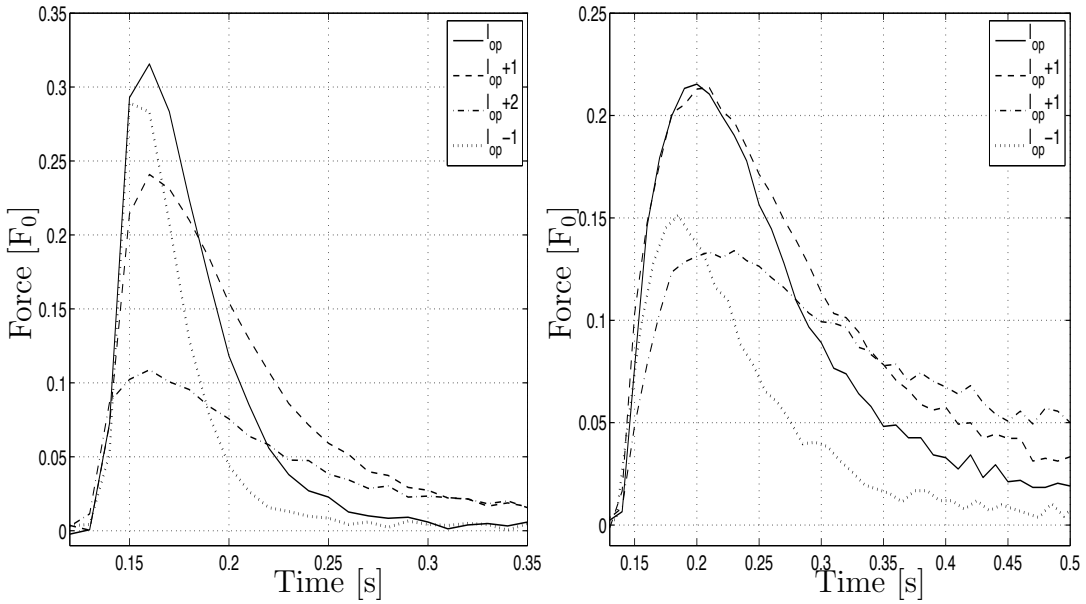

Figure 2.2: Examples of single twitch of EDL (left) and SOL (right) muscles measured at different lengths. These lengths were l_{op}, $l_{op}+1$, $l_{op}+2$ and $l_{op}-1$ mm belonging to curves (−), (–), (-.) and (..) respectively. Note the different time and force scales in the two plots.

Table 2.3: Contraction and half relaxation times of EDL at different lengths.

Contraction times [ms]							
$l - l_{\text{op}}$ [mm]	EDL − 1	EDL − 2	EDL − 3	EDL − 4	EDL − 5	EDL − 6	Mean ± STD
−1	20.0	27.5	25.0	19.6	25.8	32.5	25.1 ± 4.8
0	20.0	30.0	25.0	25.0	25.8	22.5	24.7 ± 3.4
+1	27.5	32.5	32.5	25.0	28.5	30.0	29.3 ± 2.9
+2	30.0	35.0	32.5	32.2	33.3	32.5	32.6 ± 1.6
Half relaxation times [ms]							
−1	27.5	30.0	30.0	23.2	18.2	20.0	24.8 ± 5.1
0	22.5	37.5	50.0	37.5	28.8	35.0	35.2 ± 9.3
+1	35.0	55.0	62.5	58.9	40.9	40.0	48.7 ± 11.5
+2	47.5	70.0	60.0	44.6	57.6	55.0	55.8 ± 9.1

Table 2.4: Contraction and half relaxation times of SOL at different lengths.

Contraction times [ms]						
$l - l_{\text{op}}$ [mm]	SOL − 1	SOL − 3	SOL − 4	SOL − 5	SOL − 6	Mean ± STD
−1	65.2	63.0	20.0	85.0	30.8	52.8 ± 26.7
0	82.6	63.0	30.0	90.0	57.7	64.7 ± 23.5
+1	82.6	66.7	27.5	90.0	69.2	67.2 ± 24.2
+2	73.9	92.6	45.0	105.0	76.9	78.7 ± 22.6
Half relaxation times [ms]						
−1	52.2	66.7	25.0	50.0	69.2	52.6 ± 17.6
0	78.3	66.7	25.0	105.0	76.9	70.4 ± 29.1
+1	95.7	70.4	37.5	110.0	111.5	85.0 ± 31.3
+2	187.0	77.8	47.5	160.0	184.6	131.4 ± 64.5

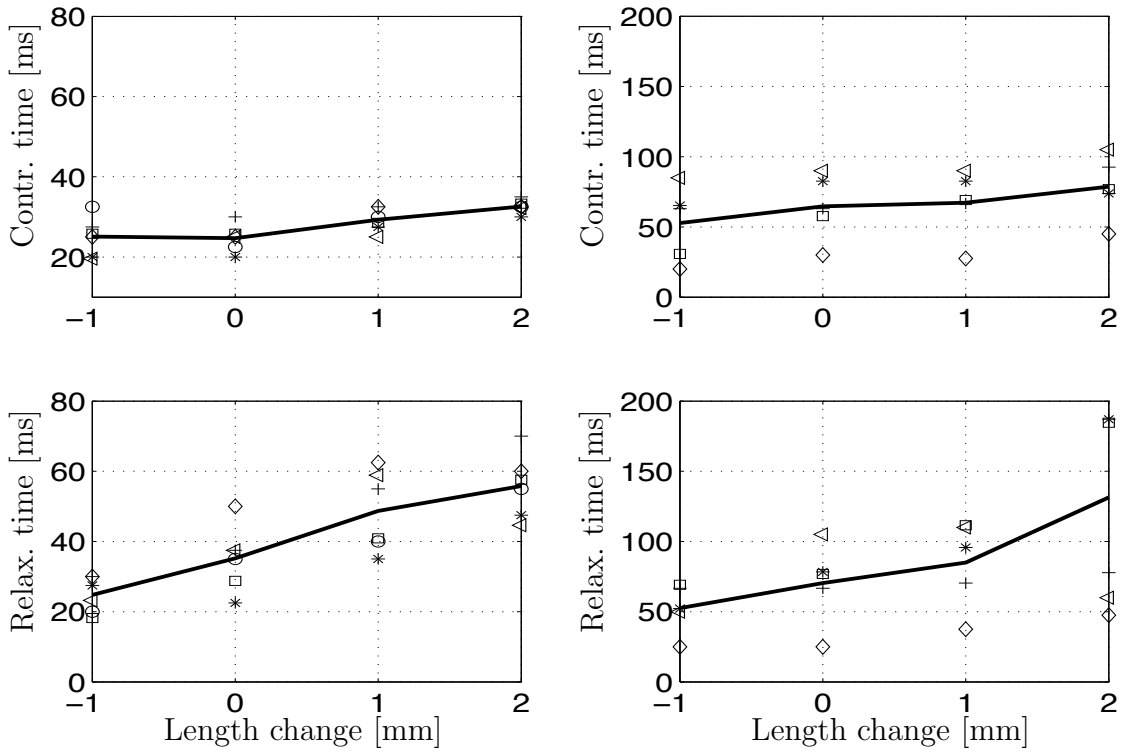

Figure 2.3: The contraction (upper) and half relaxation (lower) times as a function of muscle length change of EDL (left) and SOL (right) muscles. Length change measured from optimum length. Note the different time and force scales of the two muscles.

2.4.2 Isometric tests, variable activation

Isometric stimulations were performed on the muscles, with variable stimulation frequencies f_s. These were performed for all specimens, using the individual optimum lengths l_{op} as baseline. In these experiments, the length of the specimens were kept at their individual optimum lengths, l_{op}, cf. Tables 2.1 and 2.2. For EDL muscles, the tested stimulation frequencies were $20 \leq f_s \leq 120$ Hz and the train duration $t_s = 600$ ms. Corresponding values for SOL muscles were $10 \leq f_s \leq 100$ Hz and $t_s = 1000$ ms.

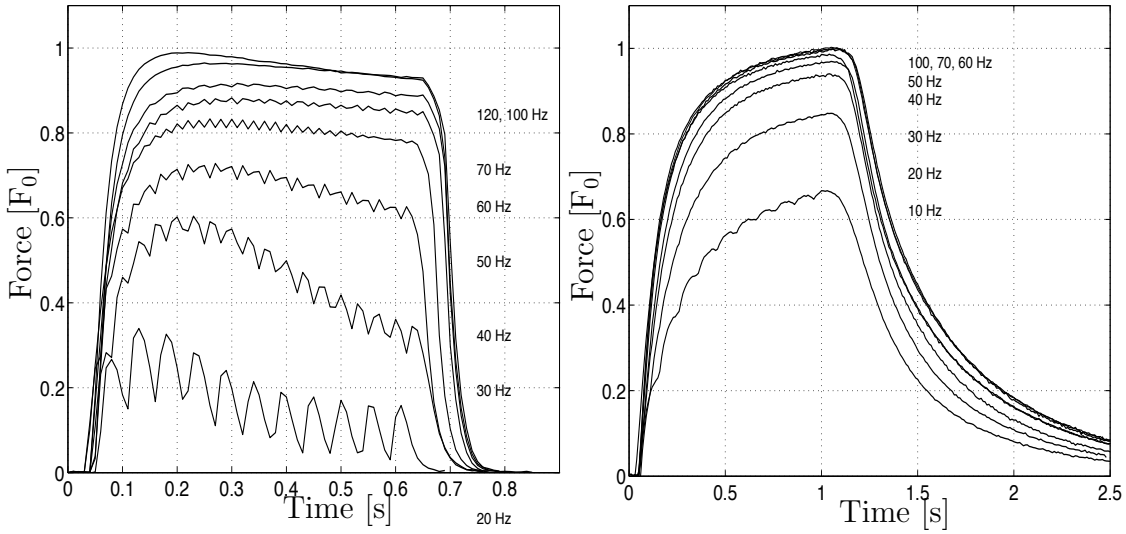

Figure 2.4: Example of experimental measurements of isometric force F at different stimulation frequencies f_s. The left panel represents EDL-1 muscle while the right panel represents SOL-1 muscle. The maximum force F_{max} was 0.33 N and 0.13 N respectively.

It was concluded that for the EDL muscles, no distinguishable further increase of the force was to be obtained if the stimulation frequency was increased beyond $f_s \geq f_t = 120$Hz. For the SOL muscles, the corresponding tetanic stimulation frequency was judged to be $f_t = 100$Hz.

Experimental time-force results from example EDL and SOL muscles are given in Fig. 2.4. All tested muscles showed very similar results. The forces were scaled to the individual maximum forces, Tables 2.6–2.7.

The results from these tests gave information on the force obtained from the muscle at tetanic stimulation, and the time needed to reach this maximum force. It also gave information on a stimulation frequency, $f_{0.5}$, needed to obtain half the maximum tetanic force.

2.4.3 Isometric contractions, variable length and activation

A series of isometric experiments were performed, with different lengths of the muscle, and different levels of activation. Tests were performed for all muscles. Stimulation was introduced at the frequencies $f_{0.5}$ and f_t from the experiments above. Also passive forces were evaluated. The muscles were stimulated at lengths of $l_{op} - 3 \leq l \leq l_{op} + 2\,\text{mm}$.

The measured passive forces at different implied lengths are shown in Table 2.5, as mean values and standard deviations within each muscle type. The values are here given as absolute force values. In order to compare the behaviors of all muscles, the facts that the muscles had very similar optimum lengths was utilized to represent

Table 2.5: Averaged passive forces of EDL and SOL muscles, at implied lengths. Forces are absolute values and lengths are given as deviations from optimum length, according to Eq. (2.3). Mean values and standard deviations for the groups.

EDL		SOL	
l^*	$F[N]$	l^*	$F[N]$
0.68	0.002 ± 0.000	0.68	0.003 ± 0.001
0.79	0.002 ± 0.001	0.79	0.003 ± 0.001
0.89	0.003 ± 0.000	0.89	0.004 ± 0.002
1.00	0.005 ± 0.001	1.00	0.008 ± 0.003
1.11	0.013 ± 0.007	1.11	0.020 ± 0.010
1.21	0.059 ± 0.025	1.21	0.055 ± 0.028

the relative length as

$$l^* = \frac{l - l_{\text{op}}}{l_{\text{op}}^{\text{av}}} + 1 \tag{2.3}$$

where l_{op}^{av} is the group average optimum lengths from Tables 2.1–2.2. For activated muscles, total forces at different lengths were registered. The individual passive forces at the lengths, for which the averages are given in Table 2.5, were subtracted from the registered force values to give active forces. In these experiments, the forces for stimulation $f_{\text{s}} = f_{\text{t}}$ and $l = l_{\text{op}}$ gave slightly different values than the F_0 obtained in the preliminary investigation. In particular, a force F_0 was obtained, Tables 2.6–2.7. This force, which for the tetanic case always occurred at $l = l_{\text{op}}$, is used for normalization in the sequel. All results for maximally stimulated muscles could, with high degree of explanation, be fitted with a third degree polynomial in the length variable. The maximum point of this function deviated only slightly from the point $(l_{\text{op}},\ F_0)$.

The individual tetanized active forces at the chosen lengths are given in Tables 2.6–2.7, normalized with respect to F_0. For the lower activation level, $f_{0.5}$, a slightly longer length tended to give a higher force, Tables 2.8–2.9. Averaged force-length curves as functions of stimulation frequency are given in Fig. 2.4, with a relative length measure l^* as abscissa, Fig. 2.5.

Table 2.6: Experimental data of active (excluding the passive part) force-length relationship of EDL muscles tetanically stimulated, with $f_t = 120$ Hz.

	Force $[F_0]$							
$l - l_{\text{op}}[$ mm]	EDL-1	EDL-2	EDL-3	EDL-4	EDL-5	EDL-6	EDL-7	Mean±STD
-3	0.215	0.218	0.185	0.129	0.449	0.0260	0.036	0.180 ± 0.143
-2	0.676	0.681	0.575	0.534	0.720	0.246	0.252	0.526 ± 0.200
-1	0.959	0.943	0.926	0.930	0.994	0.785	0.761	0.900 ± 0.090
0	1.000	1.000	1.000	1.000	1.000	1.000	1.000	1.000 ± 0.000
$+1$	0.867	0.855	0.875	0.786	0.742	0.933	0.889	0.850 ± 0.065
$+2$	0.655	0.545	0.645	0.524	0.405	0.883	0.634	0.613 ± 0.148
F_0[N]	0.328	0.336	0.337	0.263	0.244	0.314	0.377	0.314 ± 0.051

Table 2.7: Experimental data of active (excluding the passive part) force-length relationship of SOL muscles, tetanically stimulated, with $f_t = 100$ Hz.

	Force $[F_0]$							
$l - l_{\text{op}}[$ mm]	SOL-1	SOL-2	SOL-3	SOL-4	SOL-5	SOL-6	SOL-7	Mean±STD
-3	0.342	0.297	0.484	0.167	0.536	0.270	0.591	0.384 ± 0.156
-2	0.715	0.672	0.856	0.536	0.823	0.470	0.852	0.703 ± 0.155
-1	0.943	0.916	0.992	0.855	0.986	0.827	0.990	0.930 ± 0.067
0	1.000	1.000	1.000	1.000	1.000	1.000	1.000	1.000 ± 0.000
$+1$	0.873	0.909	0.712	0.899	0.823	0.858	0.759	0.833 ± 0.074
$+2$	0.566	0.672	0.332	0.529	0.532	0.670	0.404	0.529 ± 0.127
F_0[N]	0.131	0.155	0.129	0.114	0.119	0.173	0.109	0.133 ± 0.023

Table 2.8: Experimental data of active (excluding the passive part) force-length relationship of EDL muscles stimulated with $f_{0.5} = 20$Hz.

	Force $[F_0]$							
$l - l_{\text{op}}[$ mm]	EDL-1	EDL-2	EDL-3	EDL-4	EDL-5	EDL-6	EDL-7	Mean±Std
-3	0.000	0.003	0.000	0.002	0.002	0.000	0.000	0.001 ± 0.001
-2	0.075	0.076	0.057	0.072	0.138	0.003	0.015	0.062 ± 0.045
-1	0.216	0.281	0.135	0.370	0.218	0.110	0.136	0.209 ± 0.093
0	0.317	0.497	0.395	0.589	0.394	0.287	0.444	0.418 ± 0.104
$+1$	0.504	0.554	0.460	0.509	0.350	0.445	0.526	0.477 ± 0.067
$+2$	0.372	0.312	0.336	0.304	0.178	0.404	0.337	0.320 ± 0.072

Table 2.9: Experimental data of active (excluding the passive part) force-length relationship of SOL muscles stimulated with $f_{0.5} = 10$ Hz.

	Force $[F_0]$							
$l - l_{\text{op}}$[mm]	SOL-1	SOL-2	SOL-3	SOL-4	SOL-5	SOL-6	SOL-7	Mean±STD
-3	0.049	0.017	0.095	0.025	0.179	0.076	0.224	0.095 ± 0.079
-2	0.193	0.113	0.294	0.086	0.407	0.261	0.386	0.249 ± 0.125
-1	0.372	0.286	0.448	0.249	0.550	0.350	0.566	0.403 ± 0.123
0	0.569	0.500	0.546	0.511	0.668	0.500	0.705	0.571 ± 0.311
$+1$	0.681	0.556	0.440	0.667	0.571	0.626	0.557	0.585 ± 0.082
$+2$	0.469	0.401	0.206	0.509	0.365	0.496	0.273	0.388 ± 0.115

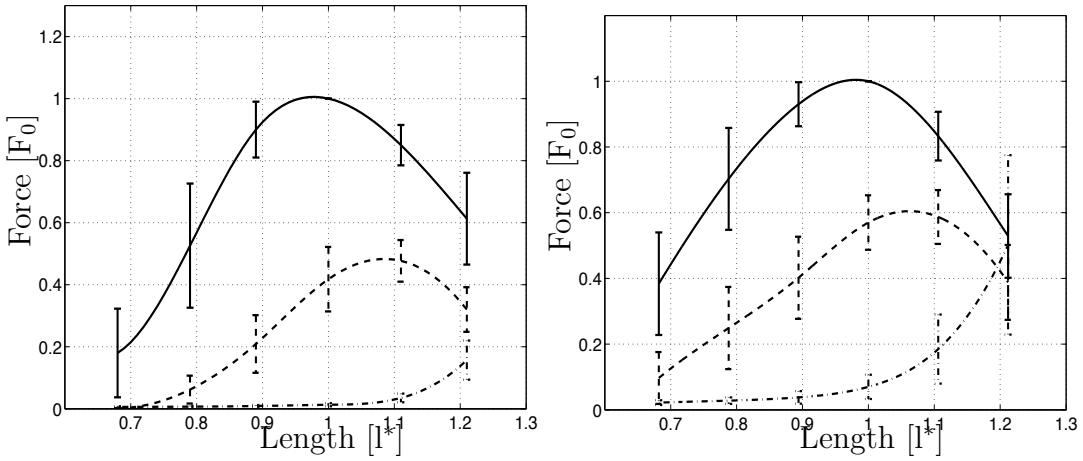

Figure 2.5: Average and standard deviation in active and passive forces of EDL (left) and SOL (right) muscles. EDL muscle was stimulated with $f_{\text{t}} = 120$ Hz and $f_{0.5} = 20$ Hz while SOL muscle was stimulated with $f_{\text{t}} = 100$ Hz and $f_{0.5} = 10$ Hz

2.4.4 Concentric case, variable velocity and pre-activation

Concentric contraction experiments were performed on *pre-activated* muscles. In this context, 'pre-activation' is defined as the activation duration of the muscles before shortening or stretch is introduced. The muscles were first maximally stimulated at $l = l_{\text{i}} = l_{\text{op}} + 0.48$ mm. With two different pre-activations, $t_0 - t_1$, the muscles were prescribed to shorten with a constant velocity to a final length, at which they were again held isometrically; the stimulation was constant throughout the experiments, cf. Fig. 2.1. EDL and SOL muscles were stimulated with $f_t = 120$ Hz and $f_t = 100$ Hz respectively. A length change $l_r = -0.48$ mm was implied over time durations between 0.20 and 0.01 s, leading to velocities between $v_r = -2.40$ and $v_r = -48.00$ mm/s, or shortenings of approximately 0.25 to 5.00 l_{op}/s.

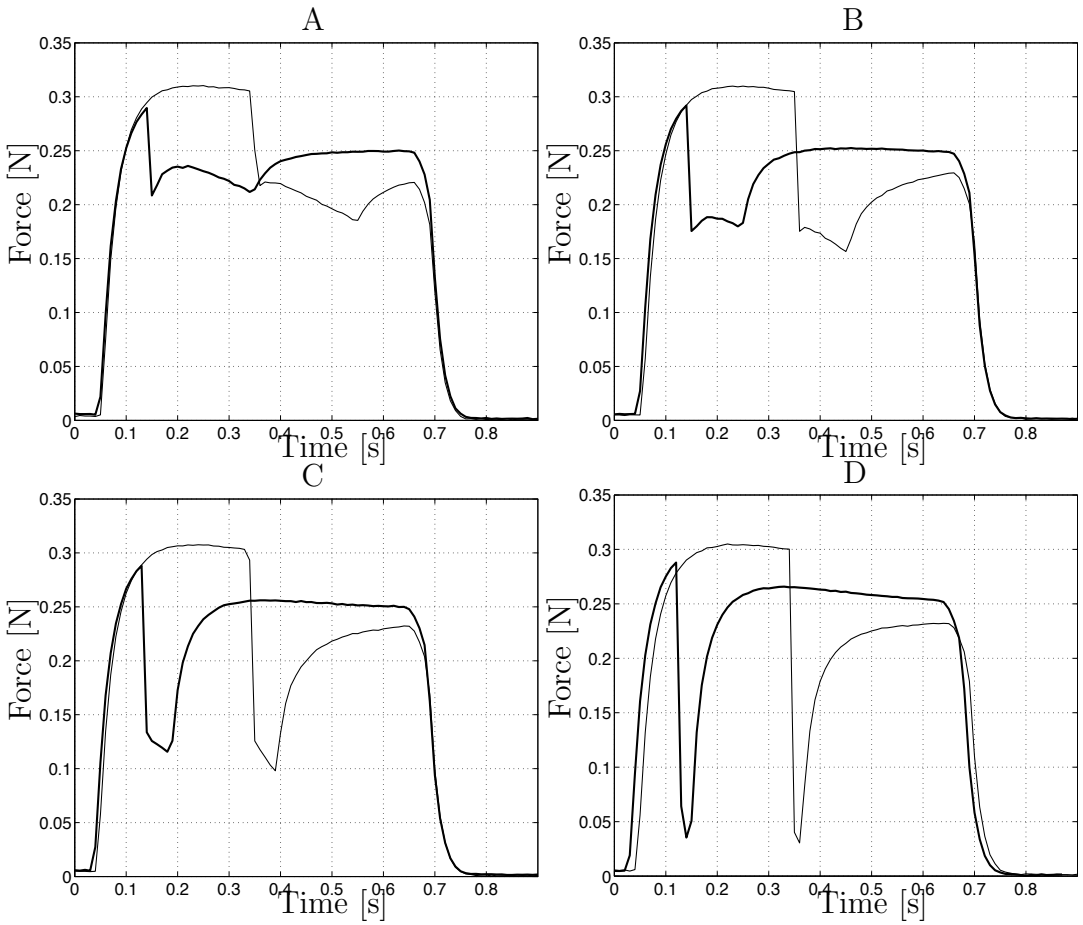

Figure 2.6: Example of concentric contraction experiments on maximally stimulated EDL muscle, with 0.10 s and 0.30 s of pre-activations and shortening velocities: (A) 0.26 l_{op}/s; (B) 0.51 l_{op}/s; (C) 1.03 l_{op}/s and (D) 2.57 l_{op}/s. The optimum length of this muscle was 9.35 mm.

EDL was pre-activated for either $t_0 - t_1 = 0.10$ s or $t_0 - t_1 = 0.30$ s and SOL muscle for either $t_0 - t_1 = 0.10$ s or $t_0 - t_1 = 0.60$ s. Typical example results are given in Figs. 2.6 and 2.7.

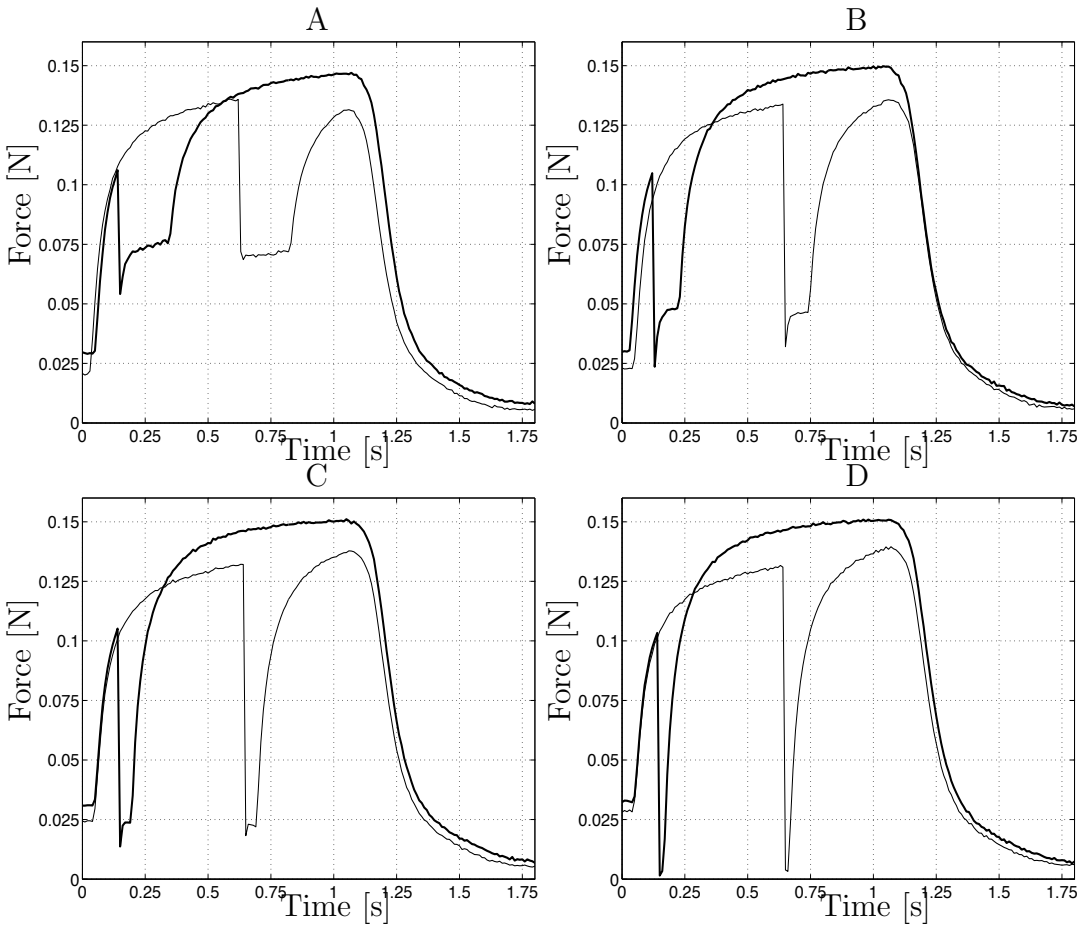

Figure 2.7: Example of concentric contraction experiments on maximally stimulated SOL muscle, with 0.10 and 0.60 s of pre-activations and shortening velocities: (A) 0.27 l_{op}/s; (B) 0.53 l_{op}/s; (C) 1.06 l_{op}/s and (D) and 2.65 l_{op}/s. The optimum length of this muscle was 9.05 mm.

2.4.5 Eccentric case, variable velocity and pre-activation

Eccentric contraction experiments were performed on pre-activated muscles. The muscles were first maximally stimulated at $l = l_i = l_{\mathrm{op}} - 0.48$ mm. With two different pre-activations, $t_0 - t_1$, the muscles were forced to stretch with a constant stretch velocity to the optimum length, $l_r = 0.48$ mm, at which they were again held isometrically. The stimulation was constant throughout the experiments. EDL and SOL muscles were stimulated with $f_t = 120$ Hz and $f_t = 100$ Hz respectively. The time for lengthening was between $t_{\mathrm{r}} = 0.20$ and $t_{\mathrm{r}} = 0.02$ s, leading to stretch velocities between $v_{\mathrm{r}} = 2.4$ and 24 mm/s or approximately 0.25 to 2.5 $\mathrm{l_{op}}$/s. EDL was pre-activated for either $t_0 - t_1 = 0.10$ s or $t_0 - t_1 = 0.30$ s and SOL muscle for either $t_0 - t_1 = 0.10$ s or $t_0 - t_1 = 0.60$ s. Example results are given in Figs. 2.8 and 2.9.

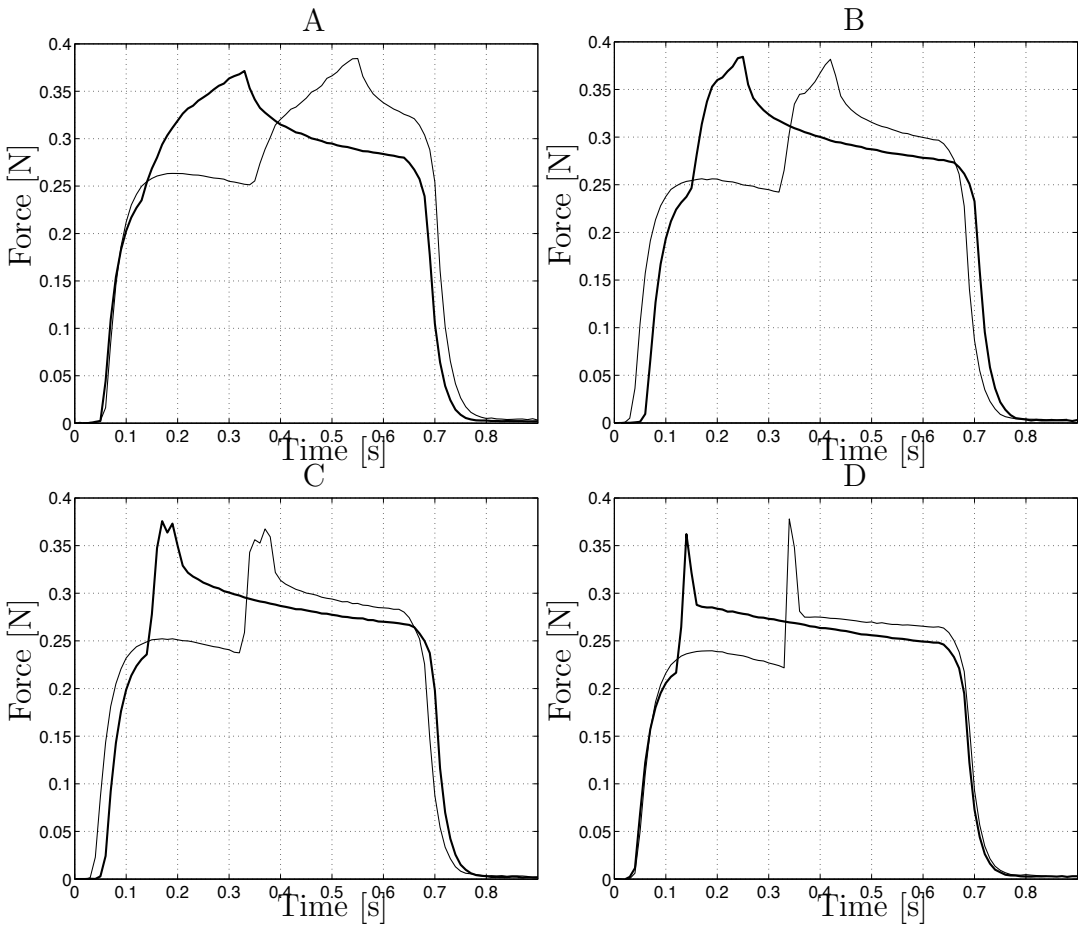

Figure 2.8: Example of eccentric contraction experiments on maximally stimulated EDL muscle, with 0.10 and 0.30 s of pre-activations and lengthening velocities: (A) 0.26 l_{op}/s; (B) 0.51 l_{op}/s; (C) 1.03 l_{op}/s and (D) 2.57 l_{op}/s. The optimum length of this muscle was 9.35 mm.

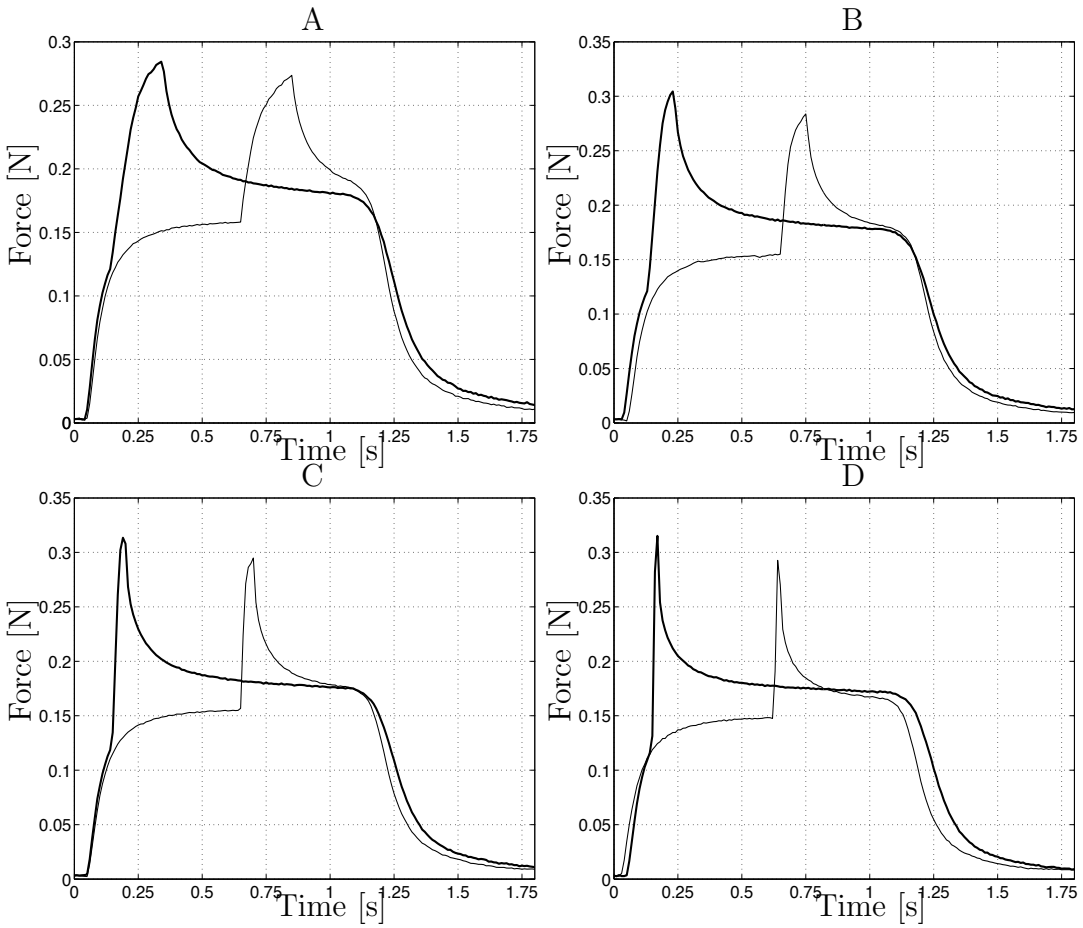

Figure 2.9: Example of eccentric contraction experiments on maximally stimulated muscle SOL-6, with 0.10 s and 0.60 s of pre-activations and lengthening velocities: (A) 0.27 l_{op}/s; (B) 0.53 l_{op}/s; (C) 1.06 l_{op}/s and (D) and 2.65 l_{op}/s. The optimum length of this muscle was 9.90 mm.

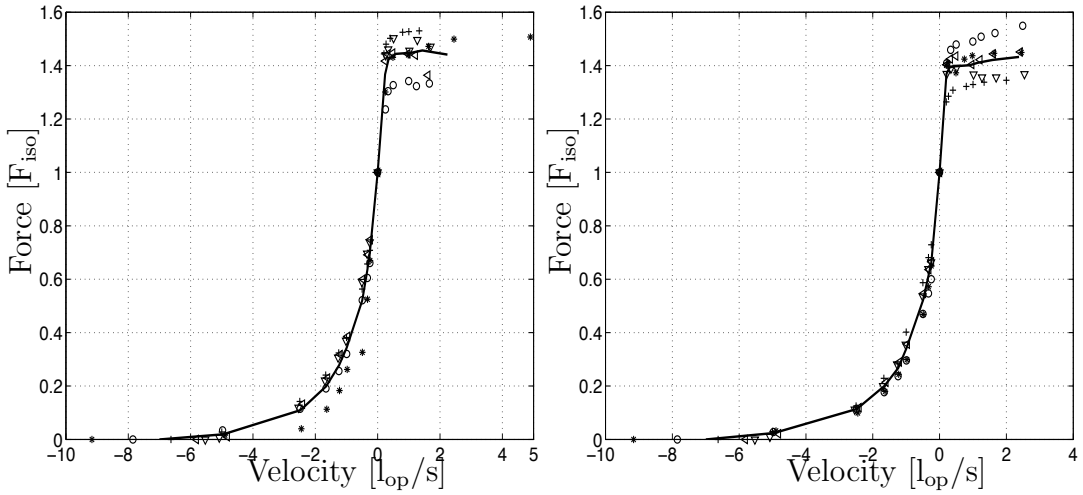

Figure 2.10: Force-velocity relationship of maximally stimulated EDL muscles with 0.1 s (left) and 0.3 s (right) of pre-activation time. The solid line represents the averaged force-velocity curve

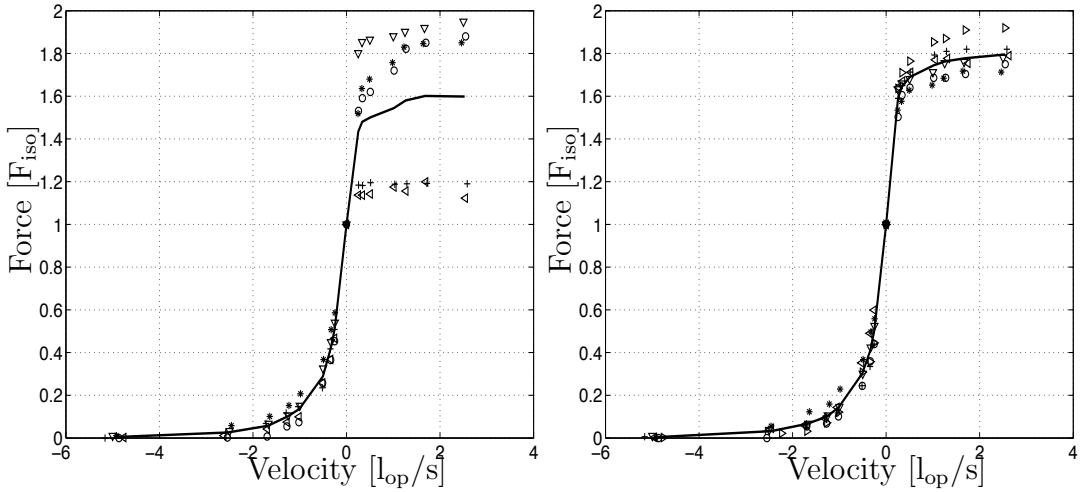

Figure 2.11: Force-velocity relationship of maximally stimulated SOL muscles with 0.1 s (left) and 0.6 s (right) of pre-activation time. The solid line represents the averaged force-velocity curve.

2.4.6 Force-velocity relationship

From performed concentric and eccentric experiments, at different pre-activations and different length change velocities, the force-velocity relationship was evaluated. The method was iso-kinetic concentric or eccentric contractions with the same amplitude and final length but different shortening or stretch velocities. The forces were related to isometric force prior to shortening or stretch, i.e., at lengths $l_{\mathrm{op}} \pm l_{\mathrm{r}}$. This force is denoted by F_{iso}. The maximum shortening velocity (v_{max}) was evaluated by

regression method. The results are shown in Figs. 2.10 and 2.11. The average curve for each muscle group corresponded to the evaluated average of experimental data for each used relative velocity.

The force-velocity relationships of EDL and SOL muscles, respectively, show different maximum shortening velocities, $v_{\max}$. In the concentric contraction, the averaged values are in good agreement with individual values, while in the eccentric contraction the dispersion of points is larger.

2.5 Discussion

The performed experiments have had as an objective to develop an experimental procedure for evaluation of muscular behavior in a more general dynamical context than the common isometric, iso-kinetic and isotonic testing paradigms. This approach is necessary for the development of simulation models for musculo-skeletal systems in movement, where the lengths and forces of muscles vary continuously, and are coupled. These effects, which have been noted in recent years, and are sometimes referred as 'history dependence', (Rassier and Herzog 2004), demand experimentation of somewhat different layout than traditional forms. The present work, although not unique, has aimed to develop a paradigm, where activation of the muscles and their length variations are independently parameterized in time. The used apparatus and parametric history have been shown to give good possibilities to study the history dependence in muscular force production for several interesting situations, with reference to a numerical modelling.

Common testing setups appear as special cases of the general paradigm. Results from these are presented above, and show mostly well-known values. A surprising result is that nominal maximum isometric force of the tested SOL muscles is consistently about 50% of that of EDL muscles. Although a common assumption is that muscles have the same nominal force capacity the finding is also supported in literature, (Fung 1993; Johansson et al. 2003).

The active force-length relations for isometric tests showed expected behaviors. With the length instances considered, no clear plateau could be seen. The relations could be well described by fitted third order polynomials.

With respect to stimulation frequencies, the SOL muscles can be considered as fully stimulated — with the used stimulation — at a lower frequency than the EDL muscles: 100 Hz compared to 120 Hz. In order to give half the maximum force, the needed stimulation frequencies were about 10 Hz and 20 Hz, respectively. As expected, maximum isometric force was obtained for longer muscle lengths with lower stimulation frequency, (Roszek et al. 1994; Stuart et al. 1998).

EDL and SOL muscles differed in their time scales, in that for isometric contractions the maximum force was reached after about 0.1 s for EDL but after 0.9 s (or, perhaps, even longer) in SOL. This delay was independent of stimulation frequency, and agrees with Stuart et al. (1998) and Zuubier et al. (1998).

The experiments were primarily seen as a starting point for measurements of force production in a dynamical context, where stimulation and length vary over time. Preliminary experiments were performed, and showed the expected history effects. Shortening under stimulation, commonly denoted concentric contractions, gave a reduction in produced force, *force depression*, which was dependent on shortening velocity, and which remained when the final length was kept isometrically activated. Two aspects were particularly interesting in the results. First, the produced force during shortening was essentially independent of the pre-activation time, although this — in particular for SOL — was highly affecting the force established isometrically before shortening. Second, a longer pre-activation time, i.e., the isometric stimulation before shortening, consistently gave lower force in the final isometric phase.

In comparing Figs. 2.10 and 2.11, the dispersion is more evident in SOL muscle than in EDL. In eccentric contraction, the difference in force production of the muscles is larger when the muscles are pre-activated for 0.1 s. When the muscles are pre-activated for 0.3 s (EDL) and 0.6 s (SOL), the force produced prior to shortening reaches close to maximum isometric tetanus. In pre-activating the muscles for 0.1 s, EDL produces force which is close to the maximum isometric force, whereas SOL produces much less force.

The force reduction during and after shortening was not systematically measured in the performed experiments. Neither was the force production measured in a phase after completed stimulation. The results, however, might give important information for the understanding of history effects in muscular force production.

The experiments on stretch under stimulation, 'eccentric contraction', also gave qualitative results on history effects. Compared to the shortening experiments, it is noted that the force increase, *force enhancement*, does not seem to be highly affected by the stretch velocity, but more related to the final length, and thereby rises more slowly for the lower stretch velocity. As for the shortening experiments, the force during stimulated stretch is independent of the pre-activation time. The timing chosen for the lengthening experiments gave results which do not allow even qualitative conclusions on the remaining history effects on the force in the isometric phase following lengthening.

A further conclusion from the stimulated lengthening experiments is that these experiments do damage to the specimen, (Gregory et al. 2003; Lovering et al. 2005; Proske et al. 2004). This is clearly seen from the initial and final isometric phases in Figs 2.8 – 2.9 where the force production is different, but should have been equal, for the different cases.

The performed experiments have shown qualitatively that muscular force production shows a strong history dependence, where activation and length variations affect the produced force, even without fatigue effects. In relation to ongoing discussion, this verifies that the basic Hill model, with a force-length and a force-velocity dependence without memory, is not capable of describing the force variation in a general dynamic situation.

Continued work with focus on the pre-activation of muscles, and in particular muscles during externally induced stretch. The prototype application is the stimulation of prepared or unprepared impact situations. To this end further experiments need be performed, where pre-activation is varied — also as a post-activation, with stimulation started as a reflex on lengthening — for variable lengthening schemes.

Although the planned experiments have had the above explorative objective, they are also believed to give important phenomenological information, useful for an improved understanding of the history effects in muscular force production. To this end, with coming numerical modelling efforts in mind, the experimental plan will follow terminology and testing paradigms from literature, (Herzog and Leonard 2005).

Chapter 3

Concentric contractions in mouse soleus and EDL muscle

3.1 Introduction

The functional potential of muscle is characterized by the relationship between the force that a muscle produces and its activation level, length and velocity. Since long time it has been known that muscle force depends on stimulation frequency in a sigmoidal fashion. It attains a maximal value at a certain stimulation frequency, beyond which no further increases in force are observed.

The velocity dependence of muscle force is described in two aspects. In muscle active shortening, or concentric contraction, Hill models are being widely used. To use the Hill model in circumstances where the muscle is not fully activated, it is necessary to have some input to the model representing activation. (Sandercock and Heckman 1997).

It is generally accepted, that the steady-state force following active shortening does not reach the maximum isometric force, associated with the final length. This property is typically referred to as steady-state, or residual, force depression. Force depression is known to increase with increasing shortening magnitude, (Maréchal and Plaghki 1979). Furthermore, force depression is long lasting, (Herzog et al. 1998) and is associated with a decrease in stiffness of the muscle or single fiber in force depressed compared to the isometric reference state, (Sugi and Tsuchiya 1988; Lee and Herzog 2003). Also, force depression following shortening can be abolished instantaneously by deactivating the muscle just long enough for force to drop to zero, (Herzog and Leonard 1997).

It has also been argued that force depression is directly influenced by the speed of shortening, (Maréchal and Plaghki 1979; Sugi and Tsuchiya 1988; Herzog and Leonard 1997; Morgan et al. 2000; Lee and Herzog 2003). This argument has been based on experiments in which a muscle was shortened by a given magnitude and with a given activation, but at different speeds, and the force depression was observed to consistently increase with decreasing speeds of shortening. However, for

these experimental conditions, the changes in speed of shortening would also be associated with changes in the force during shortening according to the force-velocity relationship. The mechanisms of these history-dependent phenomena are weakly understood and are the focus of intense scientific debate, (Herzog 2001).

Many studies have been performed on the force depression following muscle shortening but there is still a wide area of unknowns to be investigated, (Edman et al. 1978, 1982; Rassier et al. 2003). In the past two decades, it has been suggested repeatedly that force depression after shortening is associated with non-uniformity and dispersion of sarcomere lengths, (Edman et al. 1993; Julian and Morgan 1979; Morgan et al. 2000). Hypotheses based on novel findings have been proposed to explain history-dependent properties of muscle contraction, (Herzog et al. 2000). There is a general agreement that force depression increases with increasing magnitudes of shortening and decreases with increasing speeds of shortening, (Maréchal and Plaghki 1979; Sugi and Tsuchiya 1988; Herzog and Leonard 1997; Morgan et al. 2000).

With a general numerical muscle force description in mind, it is also noticeable that the force produced by a muscle will show a time-variation between the reduced force during the concentric contraction and reaching a steady-state isometric force at the final length. A description of this time-variation is believed to give important information on the mechanisms underlying the force reduction during and after concentric contraction. The principal figure for force production, when implying an iso-velocity situation between two isometric states is shown in Fig. 3.1. The interesting quantities are primarily the force reductions and the exponential time which can be assumed to be functions of the shortening event, and also can be believed to be related to the isometric force and time values.

The target of the present chapter was to investigate the steady-state force depression after active muscle shortening at maximum activation level and the underlying mechanisms. The description of the steady-state isometric force is based on an asymptotic force value and a time variation of the force following the concentric contraction.

Force depression was defined here in two different events, Fig. 3.1. 1. *Instant force depression*, ΔF_{idep}, which is the difference between the active force during shortening and maximum force, $F_{\max}$, of purely isometric contraction at the final length. 2. *steady-state force depression*, $\Delta F_{\mathrm{stdep}}$, which is the difference between the steady-state active force following shortening and maximum force $F_{\max}$ of purely isometric contraction at final length. All three quantities were defined as their asymptotic values over time, which is the maximum value passed before fatigue effects tend to reduce the force.

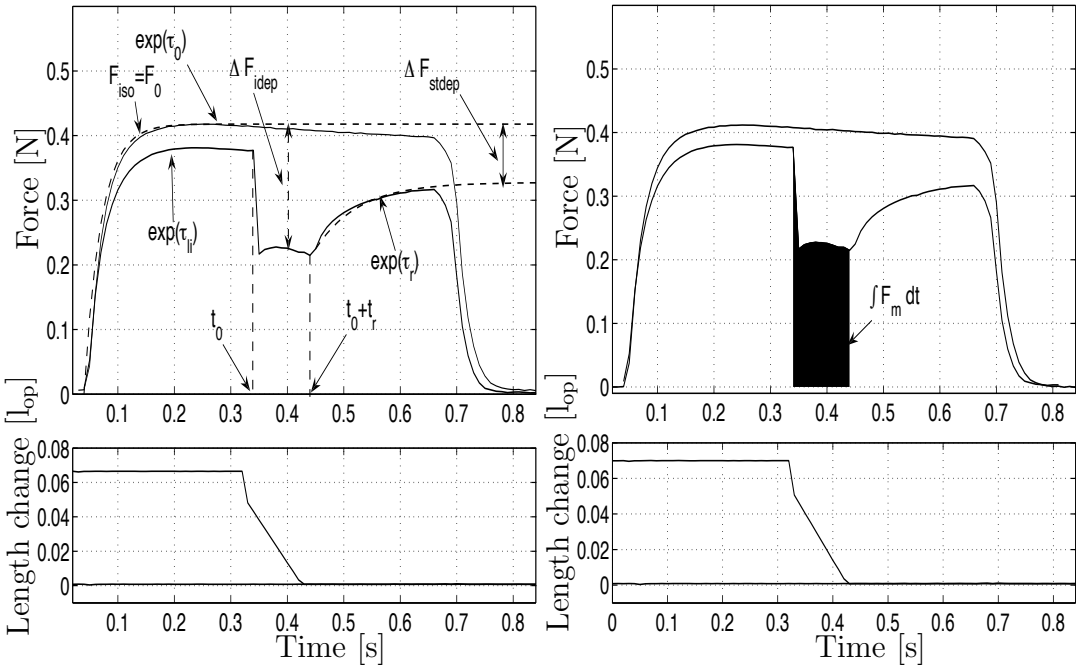

Figure 3.1: Schematic representation of isometric and concentric contractions, illustrating different features of force-time trace. The shaded part of the right panel illustrates the area of force-time trace during shortening. $\exp(\tau)$ indicates an exponential function with time constant τ. Plotted from experimental measurements of EDL.

3.1.1 Objective and scope

The present study had as its objective to study the time dependence of force production in an isometric situation following muscle shortening. The hypothesis was that there is a correlation between steady-state force depression and rise time constant of the redeveloped isometric contraction following active muscle shortening, with data from isometric testing. Steady-state force depression was assessed by comparing the steady-state isometric force produced following active muscle shortening with purely isometric reference force at the final length.

In order to test for effects of the shortening conditions on force depression, we changed the shortening speed systematically, keeping either time constant and varying the shortening magnitude, or keeping the shortening magnitude constant and varying the shortening time. The rise time constants of the early isometric phase at optimum and longer lengths and the rise time constant corresponding to post-shortening isometric force following shortening, with different shortening velocities and shortening magnitudes, were also calculated.

3.2 Materials and methods

The experiments were performed according to section 2.3.

3.2.1 Stimulation

The muscles were stimulated by rectangular current pulses of 0.5 ms duration delivered via platinum plate electrodes placed symmetrically, as closely as possible on either side of the specimen. In all experiments the stimulation voltage was ascertained to be supramaximal, 10 V. The durations of full stimulation were always $t_s = 0.60$ s for *extensor digitorum longus* ('EDL') and $t_s = 1.0$ s for *soleus* ('SOL') muscle. The applied frequencies were $f_s = 120$ Hz for EDL and 100 Hz for SOL muscle, based on preliminary experiments on the same types of muscles, Fig. 2.1

3.2.2 Paradigm

Two sets of experiments were performed on all muscles. In the first test series the shortening time, t_r, was kept constant and the shortening magnitude, l_r, was varied, (varying shortening magnitude, 'VSM'). In the second series, the shortening magnitude, l_r, was held constant and the shortening time, t_r, was varied, (varying shortening time, 'VST'). The sudden step l_{ss}, illustrated in Fig. 3.2, was introduced in order to slack the *serial elastic element*, ('SEE'), of muscle, and was released in a very short time, ~ 0.002 *á* 0.003 s. The size of the step was adjusted so that the force in the SEE at the end of the step was as close to the produced force by the *contracile element*, ('CE'), during shortening as possible.

Before active shortening was introduced, the muscles were passively lengthened by $l_r + l_{ss}$ from their optimum length, so that the shortening was initiated on the descending limb, $l_i = l_{op} + l_r + l_{ss}$, and ended at the optimum length, $l = l_{op}$, of force-length relationship.

In both methods different pre-activations were introduced. EDL muscle was pre-activated with full stimulation for either $t_0 - t_1 = 0.1$ s or $= 0.3$ s while for SOL muscle $t_0 - t_1 = 0.1$ s or $= 0.6$ s. During maximal stimulation, the muscles were then shortened and held at a fixed length for another $t_s - (t_0 - t_1) = 0.5$ s or $= 0.3$ s for EDL and $t_s - (t_0 - t_1) = 0.9$ s or $= 0.4$ s for SOL muscles, whereafter the stimulation was ended.

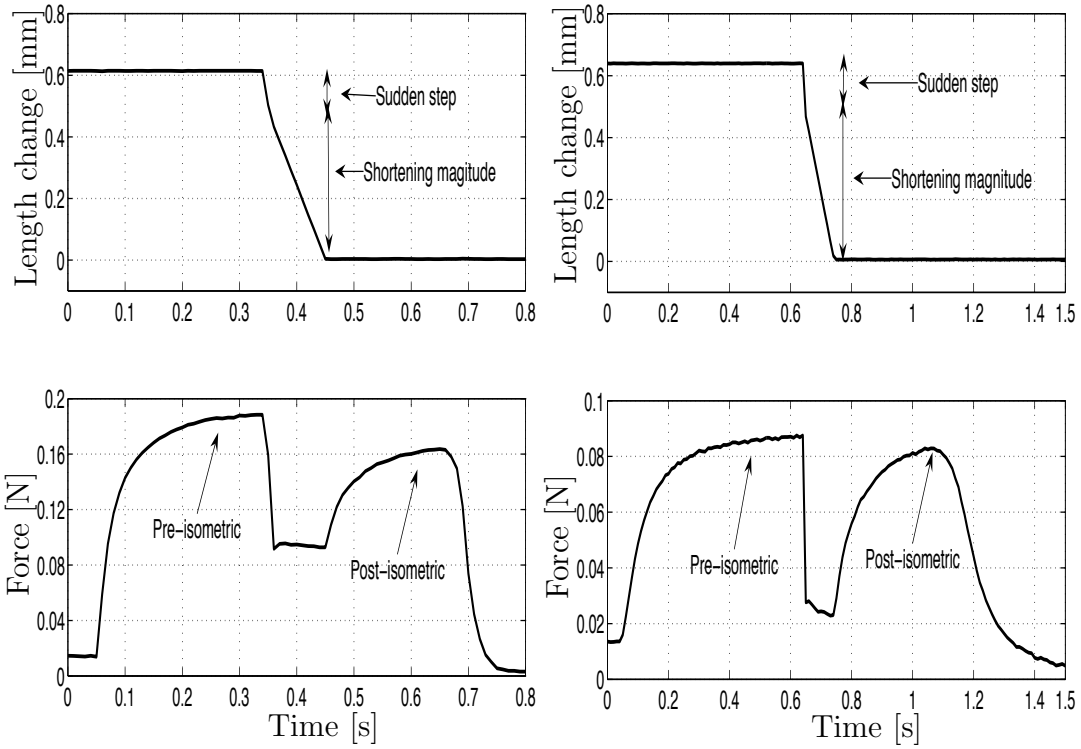

Figure 3.2: Principal results from shortening experiments, illustrating important terms, with a *sudden step* (SS), $l_{\mathrm{ss}} = 0.13$ mm. In both EDL (left panel) and SOL (right panel) muscles, the shortening magnitude $l_r = 0.48$ mm and the shortening time $t_r = 0.1$ s. The time of the SS $t_{ss} \approx 0.003$ s. Length change measured in relation to optimum length, l_{op}. Note the different time and force scales of the two muscles.

3.2.3 Experimental protocols and data analysis

All stimulation patterns and muscle puller length changes were controlled via computer, with the use of digital pulses. Obtained results were registered during experiments and stored for further analysis.

3.2.4 Evaluation procedure

The rise time constants of the redeveloped isometric contractions following shortening were calculated from the measured force-time histories in each experiment. To evaluate the time constants, the force-time trace was fitted with an exponential function. The part of the redeveloped isometric force-time trace between the end of shortening and the end of activation was considered, unless a maximum force was passed, in which case this point marked the end of the fitting interval. The evaluation gave expressions of the form

$$F(t) = F_{\mathrm{asymp}} + (F(t_0 + t_r) - F_{\mathrm{asymp}}) \exp\left(-(t - t_0 - t_r)/\tau_r\right) \tag{3.1}$$

where F_{asymp} and τ_r are results from fitting. To reach the steady-state level of the redeveloped isometric force, the fitted curve was thereby extended until a steady-state level was obtained, according to Fig. 3.1. Steady-state force depression was measured as the difference between the maximum value of the isometric force F_0 and the asymptotic redeveloped isometric force following shortening:

$$\Delta F_{\text{stdep}} = F_0 - F_{\text{asymp}} \tag{3.2}$$

Because the shortening ended at the optimum length, the redeveloped isometric force corresponds to optimum length. A similar evaluation of rise time constant was performed for the initial isometric phases at both initial length $l_{\text{op}} + l_{\text{r}} + l_{\text{ss}}$ and at final length l_{op}. These curve fittings were based on all points between the first one greater than the passive force and the last one showing an increasing value. The asymptotic value was thereby very close to the optimum force F_0 for the optimum length and a force F_{li} for the larger length l_{i}. The rise time constant for these lengths were τ_0 and τ_{li} respectively. In order to test the hypothesis from Lee and Herzog (2002) and Leonard and Herzog (2004) that steady-state force depression is related to the instant force depression during shortening, a value for instant force depression was evaluated. As the experiments show that the force production is rather far from constant during active shortening, the average force for the internal $t_0 \leq t \leq t_0 + t_{\text{r}}$ was evaluated, and the instant force depression has a form

$$\Delta F_{\text{idep}} = F_0 - \frac{1}{t_r} \int_{t_0}^{t_0+t_r} F(t)dt \tag{3.3}$$

There might also be reason to believe that the steady-state force depression is related to the mechanical work produced by the muscular force during shortening. To study this, work was evaluated for all experiments as

$$W_S = -\int_{t_0}^{t_0+t_{\text{r}}} F(t)\dot{l}dt \tag{3.4}$$

where $\dot{l}$ is the shortening velocity or time differential of length which is defined as

$$\dot{l} = -\frac{l_{\text{r}} + l_{\text{ss}}}{t_{\text{r}}}$$

As the main interest of this study is to investigate the mechanism behind force reduction during and after shortening, the mechanical work during shortening was estimated by integrating the force-time trace corresponding to the shortening period according to the right panel of Fig. 3.1 and multiplying by constant shortening velocity. Both integrals above were evaluated by a trapezoidal rule for all recorded force values in the considered intervals.

3.3 Experimental results

3.3.1 Observations

Examples of concentric contractions for the two muscle groups, and with shorter or longer pre-activations are given in Figs. 3.3 – 3.6. Each muscle experiment is thus

shown by two pairs of figures, where each pair is one prescribed length variation and one measured force variation. With the longer pre-activation times, the tetanus representing maximal sustained output the muscle can produce, was reached or almost reached before shortening was introduced. During active shortening, force rapidly decreased, and once shortening was completed, force recovered and attained a new steady-state value. This new steady-state force which was named as steady-state force depression, $\Delta F_{\mathrm{stdep}}$, was smaller than the corresponding isometric reference force, regardless of the shortening conditions and the method of muscle stimulation. It was correlated with the instant force depression, ΔF_{idep}, pre-activation time, $t_0 - t_1$ and the work, W_S, performed by the muscle during shortening. In VSM, the steady-state force depression was directly related to the instant force depression, whereas in VST these two forces were negatively correlated, Fig. 3.8. On the other hand, the instant force depression, F_{idep}, increased with increasing magnitude and speed of shortening. Consequently, the steady-state force depression following muscle shortening was directly related to the shortening magnitude. Similarly, the mechanical work performed by the muscle was increased with increasing shortening magnitude, Fig. 3.9.

The rise time constant of redeveloped isometric forces following the shortening are given in Tables 3.1 – 3.4. As the individual muscles of each type have rather similar optimum lengths, the tables give the results as functions of the group average optimal length $l_{\mathrm{op}}^{\mathrm{av}}$. The average rise time constants at the optimum length were $\tau_0 = 0.032$ s for EDL and $\tau_0 = 0.074$ s for SOL.

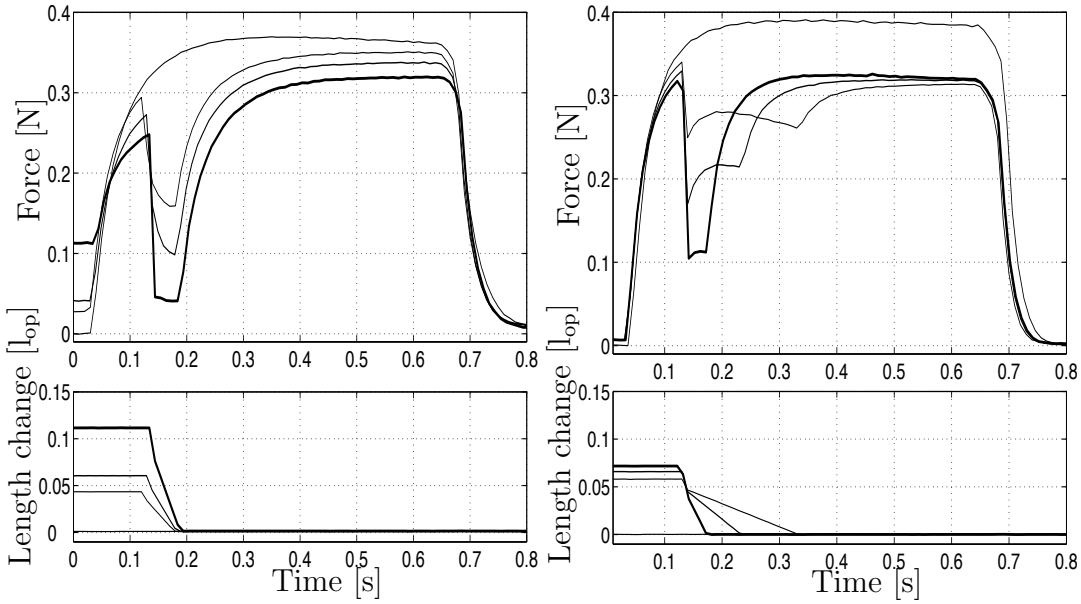

Figure 3.3: Examples of active shortening of mouse EDL muscles, $t_0 - t_1 = 0.1$ s for each measurement series. Left panel: $l_{\mathrm{r}} + l_{\mathrm{ss}} = 0.110,\ 0.061$ and $0.042\ l_{op}$ and $t_{\mathrm{r}} = 0.05$ s. Right panel: $l_{\mathrm{r}} + l_{\mathrm{ss}} = 0.072,\ 0.066$ and $0.059\ l_{\mathrm{op}}$ and $t_{\mathrm{r}} = 0.04,\ 0.10$ and 0.20 s.

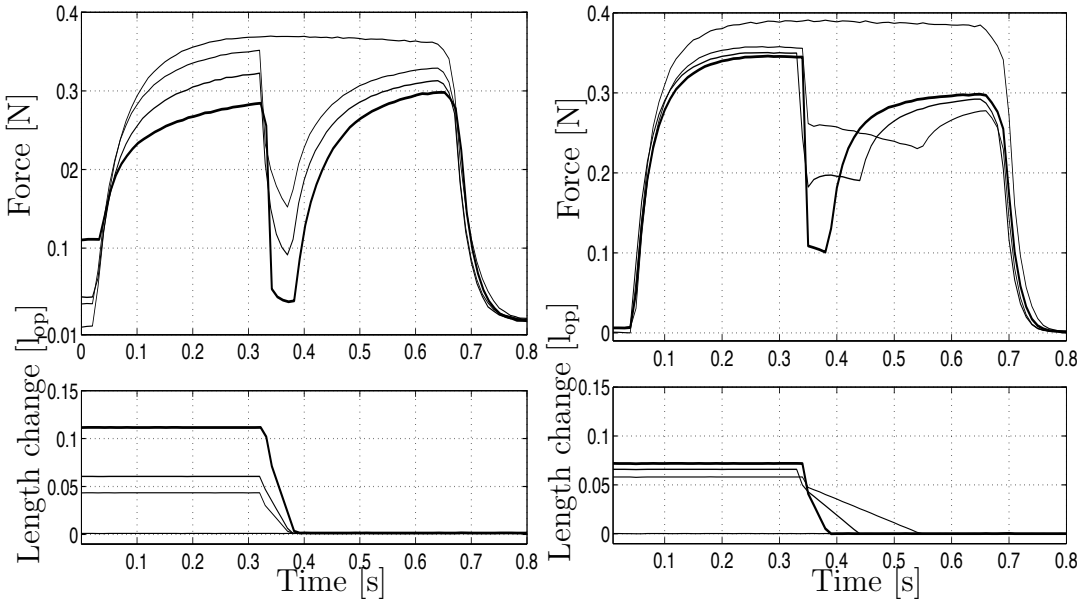

Figure 3.4: Examples of active shortening of mouse EDL muscles, $t_0 - t_1 = 0.3$ s for each measurement series. Left panel: $l_r + l_{\rm ss} = 0.110,\ 0.061$ and $0.042\ l_{op}$ and $t_{\rm r} = 0.05$ s. Right panel: $l_r + l_{\rm ss} = 0.072,\ 0.066$ and $0.059\ l_{\rm op}$ and $t_{\rm r} = 0.04,\ 0.10$ and 0.20 s.

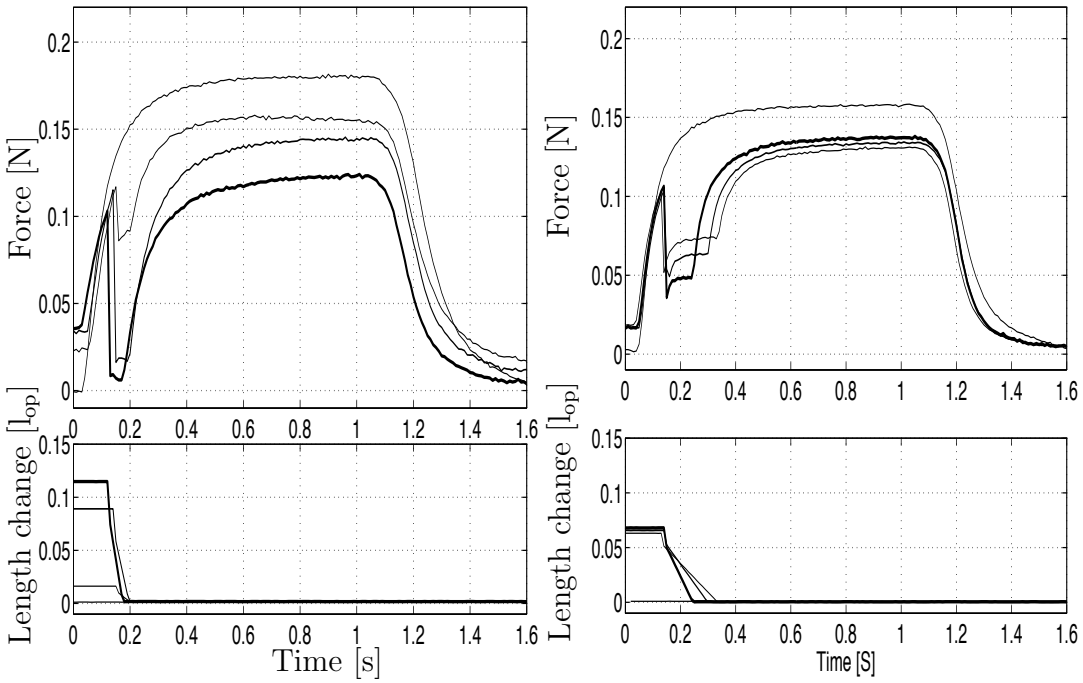

Figure 3.5: Examples of active shortening of mouse SOL muscles $t_0 - t_1 = 0.1$ s, for each measurement series. Left panel: $l_r + l_{\rm ss} = 0.113,\ 0.082$ and $0.015\ l_{\rm op}$ and $t_r = 0.05$ s Right panel: $l_{\rm r} + l_{\rm ss} = 0.066,\ 0.064$ and $0.062\ l_{op}$ and $t_{\rm r} = 0.125,\ 0.175$ and 0.200 s.

Table 3.1: Time constants of post shortening isometric contraction and steady-state force depression of maximally stimulated EDL muscle, corresponding to the VSM measurement series. Average ± standard deviation. (n = 6).

	$t_0 - t_1 = 0.1\ s$		$t_0 - t_1 = 0.3\ s$	
Short. velocity $[l_{op}^{av}/s]$	$\Delta F_{stdep}[F_0]$	τ_r [s]	$\Delta F_{stdep}[F_0]$	τ_r [s]
0.398	0.1984 ± 0.0685	0.0366 ± 0.0077	0.2251 ± 0.0590	0.0432 ± 0.0092
0.596	0.2257 ± 0.1431	0.0384 ± 0.0080	0.2421 ± 0.0712	0.0463 ± 0.0092
1.193	0.2741 ± 0.0671	0.0408 ± 0.0088	0.2754 ± 0.0654	0.0469 ± 0.0072
1.987	0.2978 ± 0.0781	0.0453 ± 0.0091	0.2911 ± 0.0711	0.0472 ± 0.0087
2.385	0.3021 ± 0.0671	0.0484 ± 0.0094	0.3051 ± 0.0812	0.0497 ± 0.0108

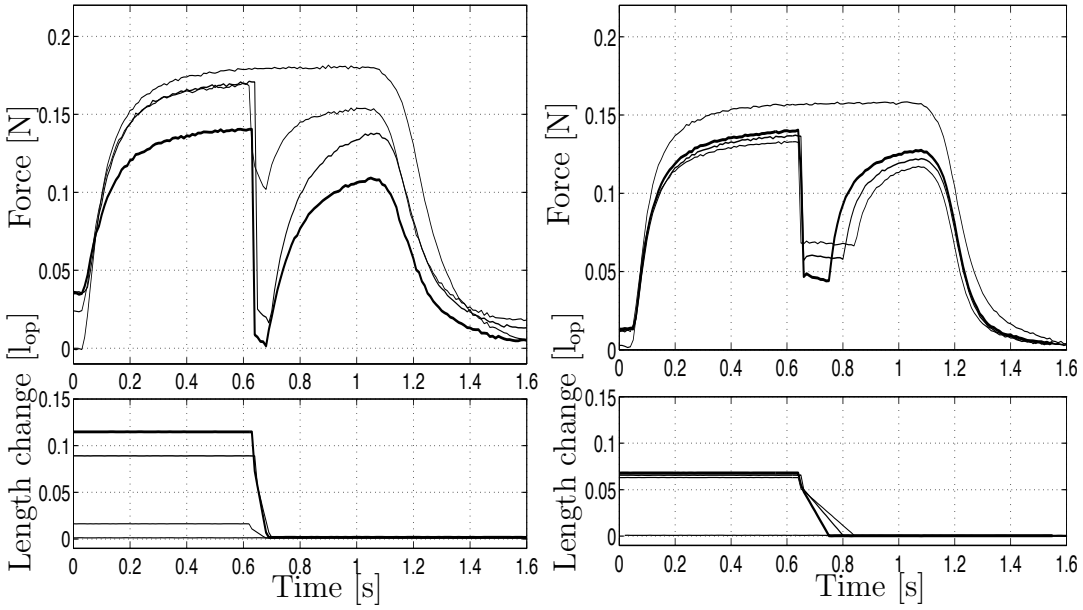

Figure 3.6: Examples of active shortening of mouse SOL muscles, $t_0 - t_1 = 0.6$ s, for each measurement series. Left panel: $l_r + l_{ss} = 0.113,\ 0.082$ and $0.015\ l_{op}$ and $t_r = 0.05$ s Right panel: $l_r + l_{ss} = 0.066,\ 0.064$ and $0.062\ l_{op}$ and $t_r = 0.100,\ 0.150$ and 0.200 s.

Table 3.2: Time constants of post shortening isometric contraction and steady-state force depression of maximally stimulated EDL muscle, corresponding to the VST mesurement series. Average ± standard deviation. (n = 6)

	$t_0 - t_1 = 0.1\ s$		$t_0 - t_1 = 0.3\ s$	
Short. velocity $[l_{op}^{av}/s]$	$\Delta F_{stdep}[F_0]$	τ_r [s]	$\Delta F_{stdep}[F_0]$	τ_r [s]
0.251	$0.2831 \pm 0,0579$	0.0509 ± 0.0077	0.3028 ± 0.0735	0.0555 ± 0.0103
0.502	$0.2487 \pm 0,0582$	0.0400 ± 0.0046	0.2887 ± 0.0675	0.0515 ± 0.0073
1.255	$0.2090 \pm 0,0630$	0.0340 ± 0.0028	0.2544 ± 0.0511	0.0405 ± 0.0040
2.511	$0.1972 \pm 0,0583$	0.0300 ± 0.0020	0.2298 ± 0.0170	0.0354 ± 0.0048

Table 3.3: Time constants of post shortening isometric contraction and steady-state force depression of maximally stimulated SOL muscle, corresponding to the VSM measurement series. Average ± standard deviation. (n = 6)

	$t_0 - t_1 = 0.1\ s$		$t_0 - t_1 = 0.6\ s$	
Short. velocity $[l_{op}^{av}/s]$	$\Delta F_{stdep}[F_0]$	τ_r[s]	$\Delta F_{stdep}[F_0]$	τ_r [s]
0.403	0.2301 ± 0.0653	0.0748 ± 0.0082	0.2565 ± 0.0736	0.0668 ± 0.0081
0.605	0.2473 ± 0.0711	0.0756 ± 0.0087	0.2808 ± 0.0781	0.0679 ± 0.0080
1.209	0.2676 ± 0.0677	0.0767 ± 0.0084	0.2991 ± 0.0784	0.0686 ± 0.0088
2.015	0.2856 ± 0.0665	0.0784 ± 0.0092	0.3138 ± 0.0767	0.0704 ± 0.0091
2.418	0.2980 ± 0.0665	0.0800 ± 0.0080	0.3185 ± 0.0711	0.0708 ± 0.0090

Table 3.4: Time constants of post shortening isometric contraction and steady-state force depression, of maximally stimulated SOL muscle, corresponding to the VST meaasurement series. Average ± standard deviation. (n = 6)

	$t_0 - t_1 = 0.1\ s$		$t_0 - t_1 = 0.6\ s$	
Short. velocity $[l_{op}^{av}/s]$	$\Delta F_{stdep}\ [F_0]$	τ_r [s]	$\Delta F_{stdep}[F_0]$	τ_r [s]
0.255	0.2875 ± 0.1629	0.0829 ± 0.0150	0.3008 ± 0.1754	0.0719 ± 0.0072
0.509	0.2772 ± 0.1640	0.0779 ± 0.0110	0.2806 ± 0.1746	0.0702 ± 0.0073
1.273	0.2616 ± 0.1680	0.0735 ± 0.0114	0.2662 ± 0.1740	0.0691 ± 0.0091
2.545	0.2584 ± 0.1613	0.0703 ± 0.0090	0.2569 ± 0.1771	0.0683 ± 0.0099

3.4 Discussion

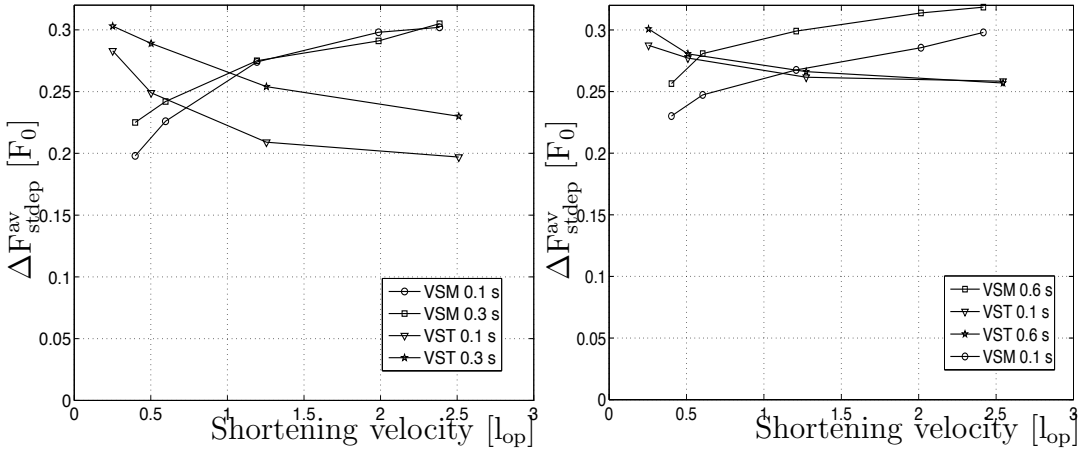

Figure 3.7: Steady-state force depression as a function of shortening velocity of EDL (left) and SOL (right) muscles. EDL muscle was pre-activated for 0.1 s or 0.3 s and SOL muscle for 0.1 s or 0.6 s. Average value for group (n = 6).

The present work has had as an object to evaluate the reliability of some proposed descriptions for steady-state force depression after active shortening. The results indicate that this force depression can not be said to be related to the shortening velocity. Fig. 3.7 shows that a statement that the force depression is positively related to the velocity is correct for our VSM experiments, where different velocities are created by varying the magnitude of shortening with a constant shortening time. The VST experiments, however, clearly contradicted such a statement. This is consistent with results observed in a variety of other muscle preparations, (Edman et al. 1978; Morgan et al. 2000; Herzog and Leonard 1997). The steady-state force depression, ΔF_{stdep}, following shortening in skeletal muscle has been associated primarily with the shortening magnitude, and the shortening speed, (Maréchal and Plaghki 1979; Sugi and Tsuchiya 1988; Herzog and Leonard 1997; Morgan et al. 2000; Lee and Herzog 2002). Our results of VST test series where the steady-state force depression was related to the speed of shortening was in good agreement with their results. The experiments also contradicted the statement that the steady-state force depression is positively correlated with the instant force depression during shortening. Again, the comparison of VSM and VST experiments shown in Fig. 3.8 indicates that this statement is true only when the shortening velocity is created by variable shortening magnitude. This result can be compared with Josephson and Stokes (1999), where a tetanically stimulated muscle from the crab, *Carcinus maenas*, was shortened by varying amounts to a common final length. The shortening, which began during the plateau of the contraction, was at constant velocity (6 mm/s), and the time of the release from isometric contraction to iso-velocity shortening was adjusted such that, in each trial, the muscle reached the final length at a fixed time following the onset of stimulation. As a result, steady-state force depression was negatively correlated

to instant force depression.

The most commonly assumed mechanism related to force depression has been sarcomere length non-uniformity, (Edman et al. 1993). For a variety of reasons, shortening speed and sarcomere length non-uniformity theory appear less interesting as candidate mechanisms at present than they might have in the past. Herzog and Leonard (1997); Herzog et al. (2000), demonstrate that force depression may vary substantially in tests in which the shortening distance and speed were kept constant and force during shortening was varied, either by altering the voltage or stimulation frequency. Furthermore, they found consistently that force depression was similar when the mechanical work performed by muscle during shortening was similar, even if the speed of shortening was changed.

The important findings from the present study were the steady-state force depression, ΔF_{stdep} dependence on instant force depression, ΔF_{idep}, mechanical work during shortening, W_S, pre-activation time, $t_0 - t_1$, and rise time constant, τ_{r}, of the redeveloped isometric contraction following the shortening.

In the VSM measurement series, the steady-state force depression increased with decreasing instant force depression, whereas in the VST measurement series, the steady-state force depression decreased with increasing instant force depression, Fig. 3.8. These results are similar to the results from Lee and Herzog (2002) where concentric contraction was performed on human *adductor pollicis* by varying the shortening magnitude.

The steady-state force depression may be associated with the amount of work performed by muscle through actin filament deformation during shortening. Work is a product of the force and shortening velocity during shortening. The results of current study indicate a positive correlation between the steady-state force depression and the mechanical work produced during active shortening regardless of the experimental method; Fig. 3.9 shows this for both muscle group. This result can be compared with Herzog et al. (2000), where it was shown that the steady-state force depression was positively related to the mechanical work produced during shortening.

With respect to activation timing, the steady-state force depression, ΔF_{stdep}, and the instant force depression, ΔF_{idep}, increased with increasing pre-activation time, Tables 3.1 – 3.4 and Fig. 3.8. One of the reasons might be the fact that during the isometric phase of each contraction prior to shortening, muscles used energy but performed no work. Thus the longer the pre-activation time the larger amount of energy was consumed during the isometric phase. This suggests that the duration of an isometric phase prior to shortening affected the steady-state force depression, ΔF_{stdep}, following the shortening and instant force depression, ΔF_{idep}, during shortening. In Figs. 3.3 – 3.6 and 3.8 there is an obvious indication that ΔF_{stdep} and ΔF_{idep} are positively correlated with $t_0 - t_1$. There is also a link between the force peak of isometric phase prior to shortening and instant force depression. In case of shorter pre-activation time, the muscle did not reach its maximum isometric force. As a consequence, the force reduction during shortening was less than in the case of longer pre-activation time where the muscle produce its maximum force, or very

close to it.

There is also a correlation between steady-state force depression following shortening and the rise time constant, τ_r, of redeveloped isometric force. In the VSM measurement series, the rise time constant increased with increasing shortening velocity (shortening magnitude), while in the VST series, it decreased with increasing shortening velocity, Tables 3.1 – 3.4. In all muscles, it was shown that the rise time constant, τ_{li}, on the descending limb, $l_i = l_{\mathrm{op}} + l_{\mathrm{r}} + l_{\mathrm{ss}}$, was greater than the rise time constant, τ_0, corresponding to optimum length. In order to let the muscles produce their maximum force before the shortening was introduced, the longer pre-activation times ($t_0 - t_1 = 0.30$ s for EDL and $t_0 - t_1 = 0.60$ s for SOL) of the muscles were considered and the rise time constant, τ_{li}, for each initial length was measured.

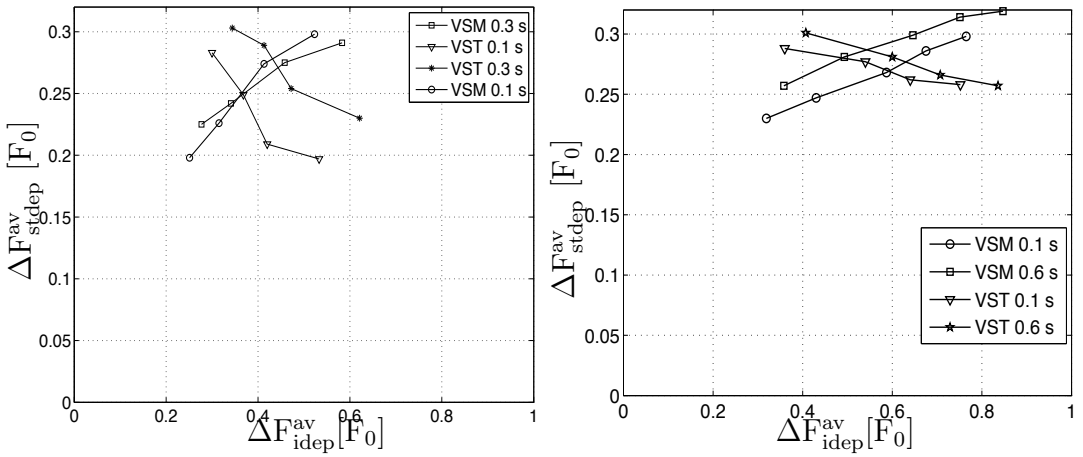

Figure 3.8: Average steady-state force depression, $\Delta F^{\mathrm{av}}_{\mathrm{stdep}}$, as a function of instant force depression, ΔF_{idep} of EDL (left) and SOL (right) muscles. EDL muscle was pre-activated for 0.1 s and 0.3 s and SOL muscle for 0.1 s and 0.6 s.

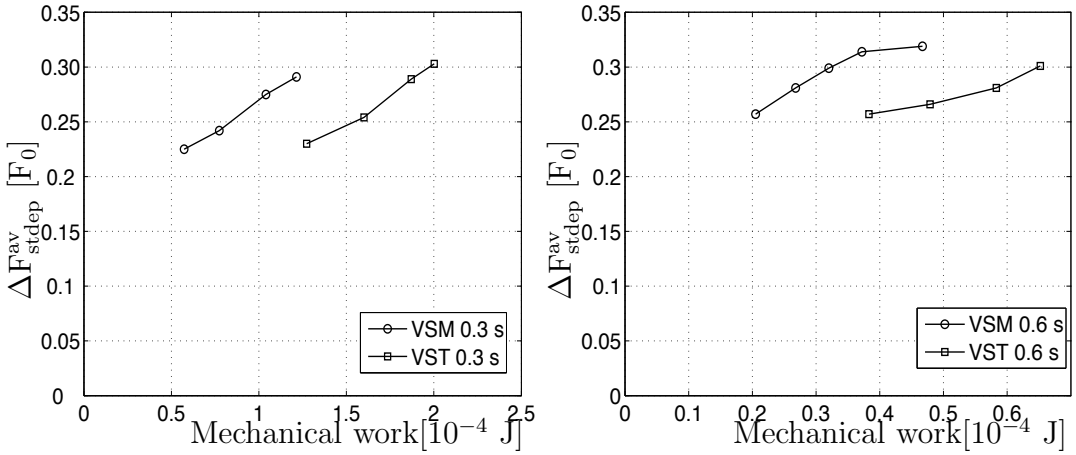

Figure 3.9: Average steady-state force depression, $\Delta F^{\text{av}}_{\text{stdep}}$, as a function of mechanical work, W_S, of EDL (left) and SOL (right) muscles pre-activated for 0.3 and 0.6 s respectively. Notice that the two plots have different scaling on abscissa.

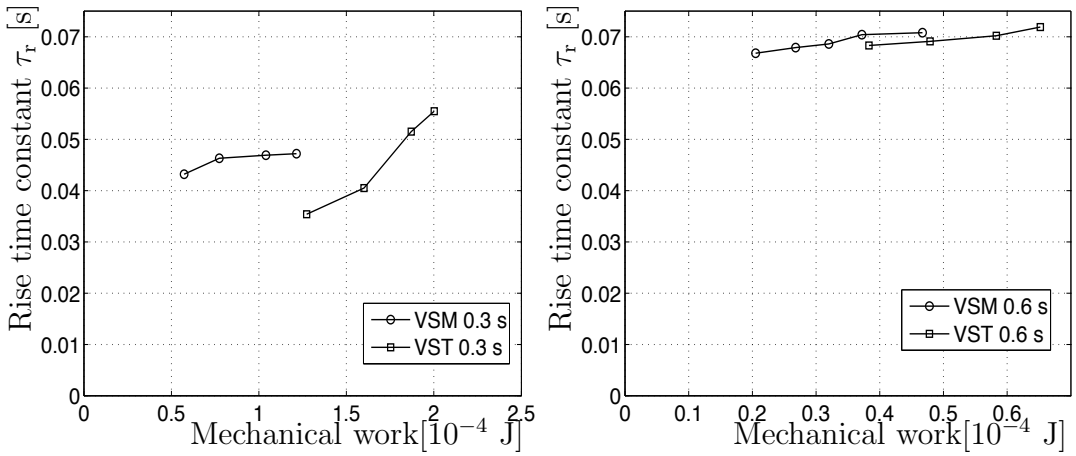

Figure 3.10: Average rise time constant of post shortening, τ_r as a function of mechanical work, W_S, of EDL (left) and SOL (right) muscles pre-activated for 0.3 and 0.6 s respectively. Notice that the two plots have different scaling on abscissa.

Chapter 4

Eccentric contractions in mouse soleus and EDL muscle

4.1 Introduction

In order to give a better understanding of the dynamic behavior of activated muscles, where external agents give rise to a time-varying length of muscle, a set of experiments were performed. These experiments were primarily focused on the behavior in stretching under activation. For this case, the term *force enhancement* is commonly used to describe that the force production in the muscle is higher than for the isometric case. For which length during the dynamic process the isometric force should be evaluated in the comparison is not consistently defined in literature.

When a skeletal muscle is first exposed to an active stretch and then held isometrically at some final length, the steady-state isometric force following the active stretch will be greater than the corresponding force obtained during a purely isometric contraction at the same final length. This phenomenon, which will be called steady-state *force enhancement* following stretch, has been observed consistently in whole muscle, (Maréchal and Plaghki 1979; Morgan et al. 2000). This property of skeletal muscle has been observed at structural levels ranging from single fibers, (Edman et al. 1978) to in vivo human skeletal muscle, (Lee and Herzog 2002).

The mechanisms responsible for force enhancement are not known. The primary explanation for force enhancement has been the development of sarcomere length non-uniformities on the descending limb of force-length relationship, (Morgan 1994; Morgan et al. 2000). However, force enhancement has been observed on the ascending limb of force-length relationship, (Edman et al. 1982; Herzog and Leonard 1997). One of the features of the sarcomere length non-uniformity theory is: There should be no force enhancement on the ascending limb of force-length relationship (Herzog 1998). Edman et al. (1978, 1982) speculated that force enhancement may be associated with the recruitment of an elastic component arranged in parallel to the contractile element, and recruited only upon activation and stretch.

Force enhancement can be accomplished if, after stretch, there is an increase in the

proportion of cross bridges attached to actin, (Herzog 1998). If this hypothesis is correct, force enhancement should be accompanied by an increase in muscle or fiber stiffness. Herzog and Leonard (2000) reported an increase in stiffness in steady-state force enhancement in cat *soleus* ('SOL'). Another theory is *engagement of a passive element hypothesis*. It has been suggested that force enhancement may be associated with the the engagement of a passive element on activation and the extension of this passive element during active stretch, (Herzog and Leonard 2002; Herzog et al. 2003). Basic equations used come from Hill (1938, 1970); Fung (1993). As pointed out by Fung, the so called Hill's model has been modified and extended over the years, and the term now seems to be used for any muscular model, in which a rheological, mechanical model is used for explanation and derivation.

The force produced by a muscle will show a time-variation between the increased force during the eccentric contraction and the steady-state isometric force reached at the final length. A description of this time-variation is believed to give important information on the mechanisms underlying the force increase during and after eccentric contraction. The principal figure for force production, when implying an iso-velocity ramp between two isometric states is shown in Fig. 4.1. The interesting quantities are primarily the force increase and the exponential time which can be assumed to be functions of the stretch event, and also can be believed to be related to the isometric force and time values.

When a muscle has been stretched, it possesses potential energy and has the ability to do work. It exerts a storing force opposite to the stretching force, (Gordon et al. 2000). Upon release, the stored energy is lost as kinetic energy and in doing friction work. The muscle together with their tendons behave as spring that absorbs and recovers elastic recoil energy. Because this function is time dependent, if the energy is not recovered, it is lost as heat. Putting these two important muscle properties together into a single model, the muscle functions like a shock absorber in series with a spring. This model includes two features of eccentric contraction: Absorption of energy and its time-dependent recovery, (Lindstedt et al. 2001). In for example, frog skeletal muscle, about 34% of the maximum absorbed energy could be stored elastically in cross-bridges, tendons, thick, thin and titin filaments and by cross-bridge states redistributions; the remaining energy could have been stored in transverse, elastic connections between myofilaments, (Linari et al. 2003).

The target of this chapter was to investigate the steady-state force enhancement following active muscle stretch and the underlying mechanisms. The description of the steady-state isometric force is based on an asymptotic force value and a time variation of the force following the eccentric contraction.

Force enhancement was defined here in two different events. 1. *Instant force enhancement*, ΔF_{ienh}, which is the difference between the maximum active force at the end of stretch and the maximum force, F_0, of a purely isometric contraction at the final length. 2. *Steady-state force enhancement*, ΔF_{stenh}, which is the difference between the steady-state active force following stretch and maximum the force, F_0, of a purely isometric contraction at final length.

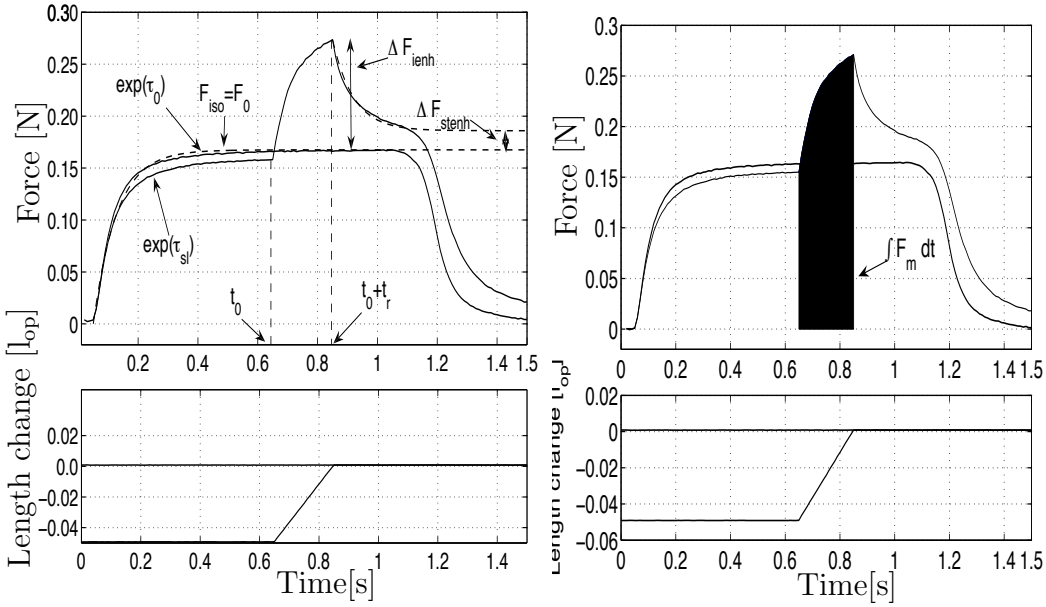

Figure 4.1: Schematic representation of isometric and eccentric contractions, illustrating different features of force-time trace. The shaded part of the right panel illustrates the area of force-time trace during stretch. $\exp(\tau)$ indicates an exponential function with time constant τ.

4.1.1 Objective and scope

The present study had as its objective to study the time dependence of force production in a steady-state situation following muscle stretch. The hypotheses was that there is a correlation between steady-state force enhancement and relaxation time (fall time) constant of the relaxed isometric contraction following muscle active stretch and values for isometric situations. Steady-state force enhancement was assessed by comparing the steady-state isometric force following active muscle stretch with the purely isometric reference force at final length.

In order to test for effects of the stretch conditions on the steady-state force enhancement, we changed the parameters systematically: keeping stretch time constant and varying the stretch magnitude in the first measurement series (Varying length magnitude, 'VLM') and keeping the stretch magnitude constant and varying the stretch duration in the second measurement series (Varying lengthening time, 'VLT'). The fall time constants of relaxation following stretch, with different stretch velocities and stretch magnitudes, were also measured.

Table 4.1: The registered and calculated data of EDL and SOL muscles. (n=6)

Parameter	EDL	SOL
l_{op} [mm]	9.56 ± 0.18	9.43 ± 0.29
Mass [mg]	13.19 ± 1.35	10.89 ± 1.34
PCSA[mm^2]	1.31 ± 0.13	1.10 ± 0.15
$F_0[N]$	0.31 ± 0.05	0.13 ± 0.02
$W_{L,max}[10^{-4}J]$	2.204 ± 0.109	1.227 ± 0.581

4.2 Materials and Methods

'Animals', 'muscle preparation and mounting', 'stimulation', and 'experimental protocols' are described in sections 2.3.1, 2.3.2, 3.2.1 and 3.2.3 respectively.

4.2.1 Paradigm

The experimental method is schematically described in Fig. 2.1, where the right half describes the activation and displacement sequences, used to allow isometric and eccentric contractions at certain stimulation frequencies, but also different timings of the activation in relation to the length variation. By choosing a suitable initial length, l_i, a stretch velocity, l_r/t_r and a pre-activation timing, described by $t_0 - t_1$, different combinations of length and stretch velocity can be obtained.

Two sets of experiments were performed on all muscles. In the first test series, the stretch magnitude, l_r, was varied and the stretch time, t_r was kept constant, VLM. In the second series the stretch magnitude, l_r, was held constant and the stretch duration, t_r was varied, VLT. Before active stretch was introduced, the muscles were passively shortened by l_r, so that the stretch was initiated on the ascending limb, $l_i = l_{op} - l_r$, and ended at the optimum length, $l_i = l_{op}$ of force-length relationship.

In both methods two different *pre-activations* were introduced. EDL muscle was pre-activated with full stimulation for either $t_0 - t_1 = 0.1$ s or $= 0.3$ s, while for SOL muscle $t_0 - t_1 = 0.1$ s or $= 0.6$ s. During maximal stimulation, the muscles were then stretched and held at a fixed length for another $t_s - (t_0 - t_1) = 0.5$ s or $= 0.3$ s for EDL and $t_s - (t_0 - t_1) = 0.9$ s or $= 0.4$ s for SOL muscles, whereafter the stimulation was ended.

4.2.2 Evaluation procedure

The fall time constants, of the relaxed isometric contractions following stretch were calculated from the measured force-time histories in each experiment. The force-time trace was fitted with an exponential function, between the end of stretch and

the end of activation. The evaluation gave expressions of the form

$$F(t) = F_{\text{asymp}} + (F(t_0 + t_\text{r}) - F_{\text{asymp}}) \exp(-(t - t_0 - t_r)/\tau_\text{f}) \tag{4.1}$$

where F_{asymp} and τ_f are results from fitting. Steady-state force enhancement was measured as the difference between the maximum value of the isometric force, F_0, and the asymptotic relaxed isometric force following stretch:

$$\Delta F_{\text{stenh}} = F_{\text{asymp}} - F_0 \tag{4.2}$$

As the experiments show that the force production is rather far from constant during active stretch, the instant force enhancement was defined from the asymptotic value F_{asymp}, when an exponential function similar to Eq. 4.1 was fitted to the lengthening phase. There might also be reason to believe that the steady-state force enhancement is related to the mechanical work produced by the muscular force during stretch. To study this, work was evaluated for all experiments as

$$W_L = -\int_{t_0}^{t_0+t_r} F(t)\dot{l}dt \tag{4.3}$$

where $\dot{l}$ is the stretch velocity or time differential of length which is defined as

$$\dot{l} = \frac{l_r}{t_r}$$

As the main interest of this study was to investigate the mechanism behind force enhancement during and after stretch, the mechanical work during stretch was estimated by integrating the force-time trace corresponding to the stretch period according to the right panel of Fig. 4.1 and multiplying by the constant stretch velocity. The integral in Eq. 4.3 was evaluated by a trapezoidal rule for all recorded force values in the considered intervals.

4.3 Experimental results

4.3.1 Observations

With low stretch velocity, muscle force rose continuously along an exponential course. At high stretch velocity, the force tended to rise continuously to a yield point, after which it continued to rise but at lower slope than previously. Examples of eccentric contractions for the two muscle types, and with shorter or longer pre-activations are given in Figs. 4.2– 4.5. Each muscle experiment is thus shown by a prescribed length variation and a measured force variation. With the longer pre-activations, the maximal sustained output the muscle can produce, occurred before stretch was introduced. During active stretch, force rapidly increased, and once stretch was completed, force relaxed and approached a new steady-state value. This new steady-state force defined as the steady-state force enhancement, ΔF_{stenh}, was greater than the isometric force of the corresponding length, regardless of the

stretch conditions and the method of muscle stimulation. It was correlated with the instant force enhancement, ΔF_{ienh}, pre-activation $t_0 - t_1$ and mechanical work, W_L, absorbed by muscle during stretch. In VLM, the steady-state force enhancement was directly related to the instant force enhancement, whereas in VLT, there was no distinct correlation between instant force enhancement, F_{ienh}, and steady-state force enhancement, F_{stenh}. The work required to stretch the muscle increased as the stretch magnitude increased and it increased with very little amount with increasing the stretch velocity, Figs. 4.2–4.5 and 4.6.

In VLM the steady-state force enhancement following muscle stretch was positively correlated with the stretch magnitude. Similarly, the mechanical work absorbed by the muscle during stretch was increased with increasing stretch magnitude. In VLT, the steady-state force enhancement was negatively correlated with the speed of muscle stretch, and for a given stretch magnitude and constant activation, mechanical work absorbed by the muscle was increased with increasing stretch velocity, Fig. 4.6.

The relaxation time constant of post-stretch isometric forces are given in Tables 4.2 – 4.5. As the individual muscles of each type have rather similar optimum lengths, the tables give the results as functions of the group average optimum length $l_{\text{op}}^{\text{av}}$.

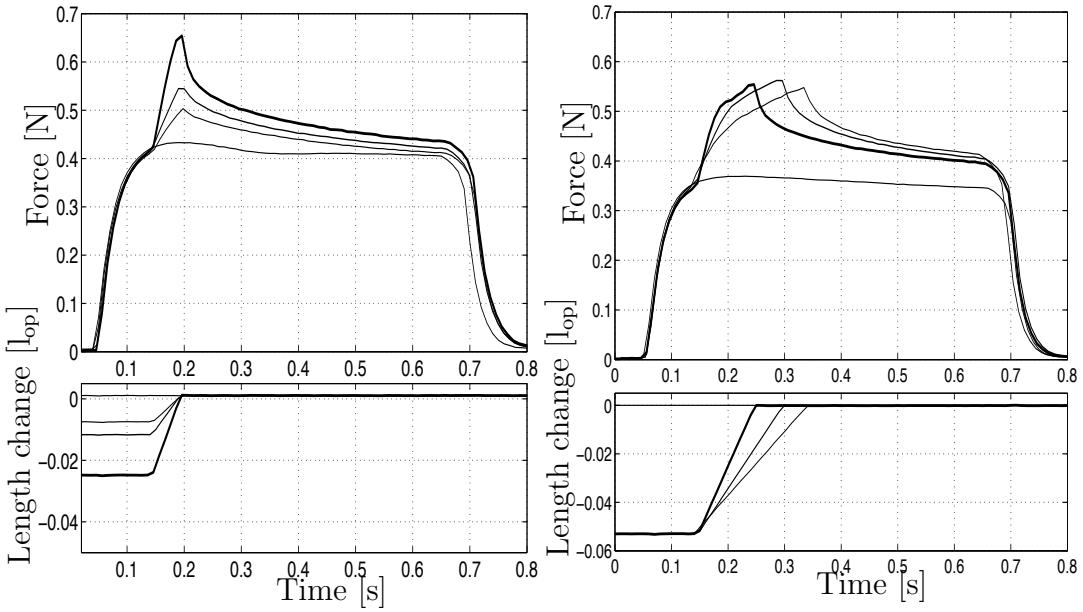

Figure 4.2: Examples of muscle stretch on ascending limb of force-length relationship of mouse EDL muscle. The muscles were pre-activated for 0.1 s. Left pair: $l_r = 0.026$, 0.013 and 0.009 l_{op} and rise time, $t_r = 0.05$ s. Right pair $l_r = 0.052$ l_{op} and rise times, $t_r = 0.20$, $=$ 0.15 and $=$ 0.10 s.

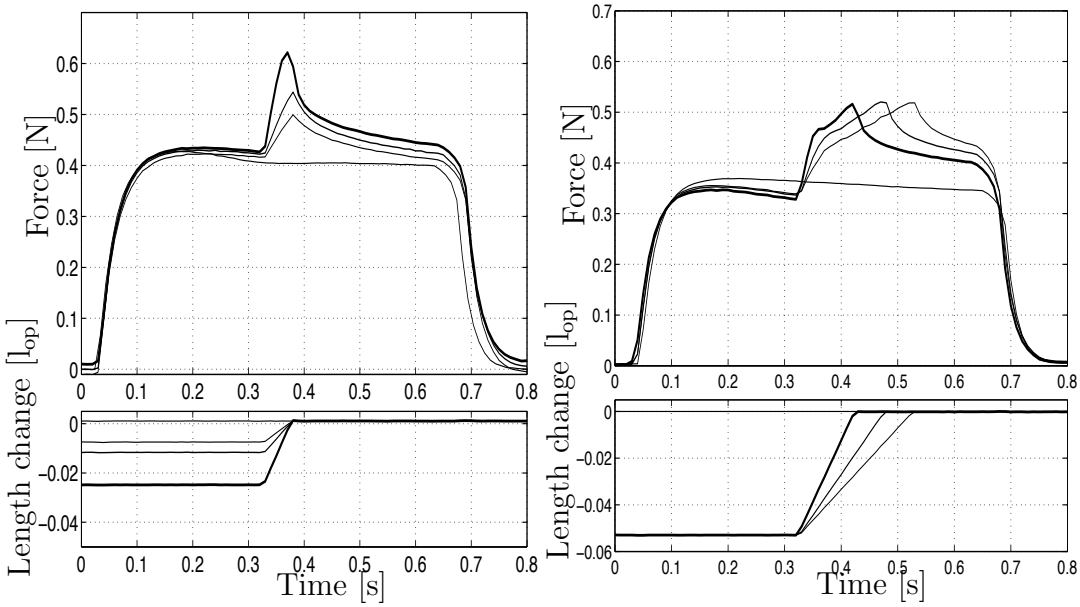

Figure 4.3: Examples of muscle stretch on ascending limb of force-length relationship of mouse EDL muscle. The muscle were pre-activated for 0.3 s. Left pair: VLM with $l_r = 0.009,\ 0.013$ and $0.026\ l_{\rm op}$ and rise time $t_r = 0.05$ s. Right pair: VLT with $l_r = 0.052\ l_{\rm op}$ and rise time $t_r = 0.20$ s, $= 0.15$ s and $= 0.10$ s.

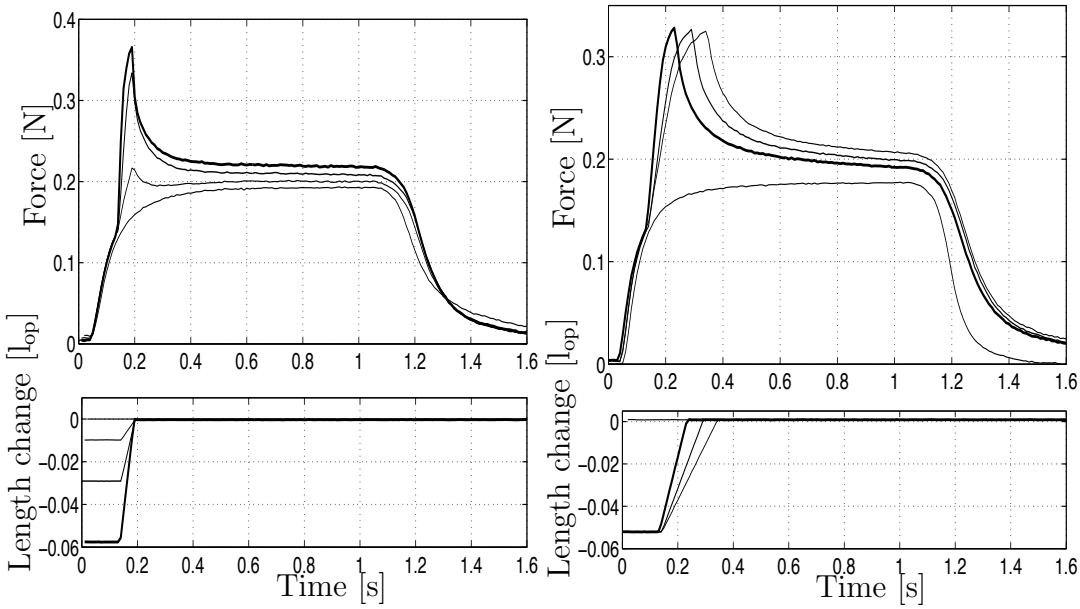

Figure 4.4: Examples of muscle stretch on the ascending limb of force-length relationship of mouse SOL muscle. The muscles were pre-activated for 0.1 s Left pair: VLM with $l_r = 0.009,\ 0.028$ and $0.055\ l_{\rm op}$, and rise time $t_r = 0.05$ s. Right pair: VLT with $l_r = 0.052\ l_{\rm op}$ and rise time $t_r = 0.2,\ = 0.15$ and $= 0.05$ s

Table 4.2: Time constants of post stretch isometric contraction and steady-state force enhancement of maximally stimulated EDL muscle, corresponding to the VLM measurement series. Average ± standard deviation. (n = 6).

	$t_0 - t_1 = 0.1$ s		$t_0 - t_1 = 0.3$ s	
Stretch velocity $[l_{op}^{av}/s]$	$\Delta F_{stenh}[F_0]$	τ_f [s]	$\Delta F_{stenh}[F_0]$	τ_f [s]
0.20	0.083 ± 0.055	0.199 ± 0.053	0.057 ± 0.053	0.085 ± 0.017
0.40	0.106 ± 0.062	0.131 ± 0.036	0.073 ± 0.062	0.068 ± 0.018
0.80	0.160 ± 0.063	0.107 ± 0.022	0.108 ± 0.066	0.044 ± 0.013
1.19	0.214 ± 0.062	0.093 ± 0.017	0.148 ± 0.080	0.036 ± 0.013
1.59	0.254 ± 0.051	0.086 ± 0.030	0.175 ± 0.085	0.033 ± 0.013

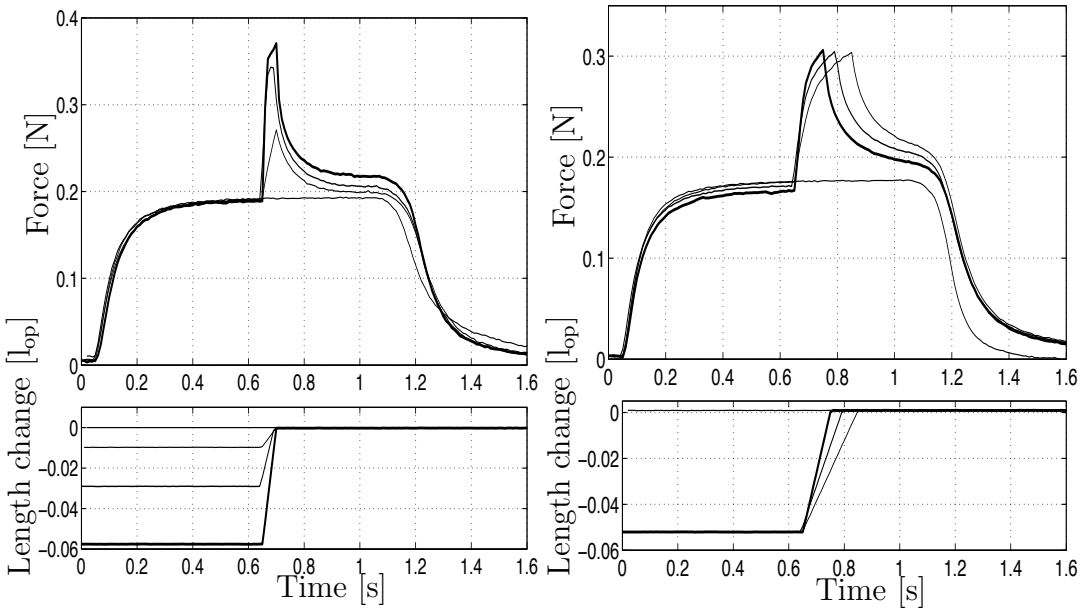

Figure 4.5: Examples of muscle stretch on the ascending limb of force-length relationship of mouse SOL muscle. The muscles were pre-activated for 0.6 s. Left pair: VLM with $l_r = 0.009$, 0.028 and $0,055$ l_{op} and rise time $l_r = 0.05$ s. Right pair: VMT with $l_r = 0.052$ l_{op} and rise time $l_r = 0.20$, $= 0.10$ and $= 0.03$ s.

4.4 Discussion

The present study has had as an object to evaluate the reliability of some proposed descriptions for steady-state force enhancement following active stretch. The results

Table 4.3: Time constants of post stretch isometric contraction and steady-state force enhancement of maximally stimulated EDL muscle, corresponding to the VLT mesurement series. Average ± standard deviation. (n = 6)

	$t_0 - t_1 = 0.1$ s		$t_0 - t_1 = 0.3$ s	
Stretch velocity $[l_{op}^{av}/s]$	$\Delta F_{stenh}[F_0]$	τ_f [s]	$\Delta F_{stenh}[F_0]$	τ_f [s]
0.25	0.125 ± 0.017	0.033 ± 0.002	0.225 ± 0.055	0.054 ± 0.016
0.34	0.081 ± 0.015	0.080 ± 0.007	0.171 ± 0.045	0.049 ± 0.005
0.50	0.062 ± 0.013	0.084 ± 0.012	0.142 ± 0.033	0.044 ± 0.007
1.00	0.041 ± 0.014	0.080 ± 0.012	0.115 ± 0.031	0.038 ± 0.006
1.26	0.031 ± 0.018	0.075 ± 0.007	0.098 ± 0.033	0.036 ± 0.006

Table 4.4: Time constants of post stretch isometric contraction and steady-state force enhancement of maximally stimulated SOL muscle, corresponding to the VLM measurement series. Average ± standard deviation. (n = 6)

	$t_0 - t_1 = 0.1$ s		$t_0 - t_1 = 0.6$ s	
Stretch velocity $[l_{op}^{av}/s]$	$\Delta F_{stenh}[F_0]$	τ_f[s]	$\Delta F_{stenh}[F_0]$	τ_f [s]
0.20	0.0400 ± 0.0166	0.037 ± 0.006	0.0400 ± 0.0127	0.046 ± 0.008
0.40	0.0514 ± 0.0149	0.034 ± 0.005	0.0504 ± 0.0143	0.038 ± 0.005
0.81	0.0670 ± 0.0199	0.030 ± 0.006	0.0599 ± 0.0124	0.034 ± 0.005
1.21	0.0864 ± 0.0231	0.027 ± 0.006	0.0698 ± 0.0083	0.027 ± 0.005
1.61	0.1074 ± 0.0235	0.023 ± 0.006	0.0794 ± 0.0059	0.023 ± 0.006

Table 4.5: Time constants of post stretch isometric contraction and steady-state force enahancement of maximally stimulated SOL muscle, corresponding to the VLT meaasurement series. Average ± standard deviation. (n = 6)

	$t_0 - t_1 = 0.1$ s		$t_0 - t_1 = 0.6$ s	
Stretch velocity $[l_{op}^{av}/s]$	$\Delta F_{stenh}[F_0]$	τ_f [s]	$\Delta F_{stenh}[F_0]$	τ_f [s]
0.26	0.1907 ± 0.0259	0.053 ± 0.019	0.1230 ± 0.0266	0.049 ± 0.009
0.34	0.1525 ± 0.0245	0.048 ± 0.020	0.1110 ± 0.0263	0.047 ± 0.008
0.51	0.1337 ± 0.0212	0.045 ± 0.020	0.1011 ± 0.0262	0.041 ± 0.010
1.02	0.1140 ± 0.0218	0.035 ± 0.021	0.0920 ± 0.0242	0.033 ± 0.011
1.27	0.1074 ± 0.0235	0.030 ± 0.011	0.0853 ± 0.0230	0.031 ± 0.011

indicate that this force enhancement can not be said to be related to the stretch velocity. Fig. 4.7 shows that a statement that the force enhancement is positively correlated to the velocity is correct for our VLM experiments, where different velocities are created by varying the magnitude of stretch with a constant stretch time. The VLT experiments, however, clearly contradicted such a statement. This observation is consistent with force enhancement observed in a variety of other muscle preparations, (Edman et al. 1978; Morgan et al. 2000).

The steady-state force enhancement, ΔF_{stenh}, following stretch in skeletal muscle has been associated primarily with the stretch magnitude, and the stretch velocity, (Maréchal and Plaghki 1979; Herzog and Leonard 1997; Morgan et al. 2000; Lee and Herzog 2002). Our results from the VLT test series where the steady-state force enhancement was related to the velocity of stretch was in good agreement with their results.

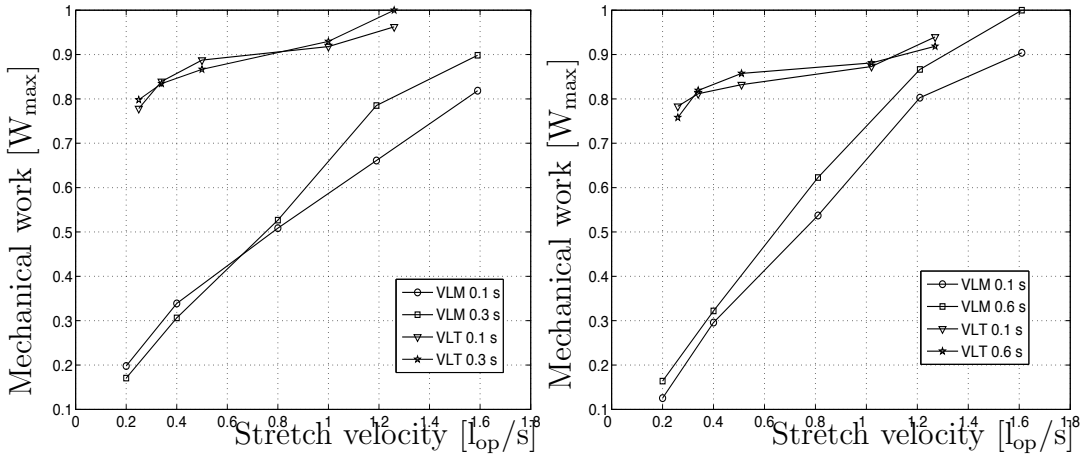

Figure 4.6: Average mechanical work as a function of stretch velocity of EDL (left) and SOL (right) muscles. EDL muscle was pre-activated for 0.1 s and 0.3 s and SOL muscle for 0.1 s and 0.6 s. Maximum mechanical work of EDL and SOL muscles were 2.204×10^{-4} J and 1.227×10^{-4} J respectively.

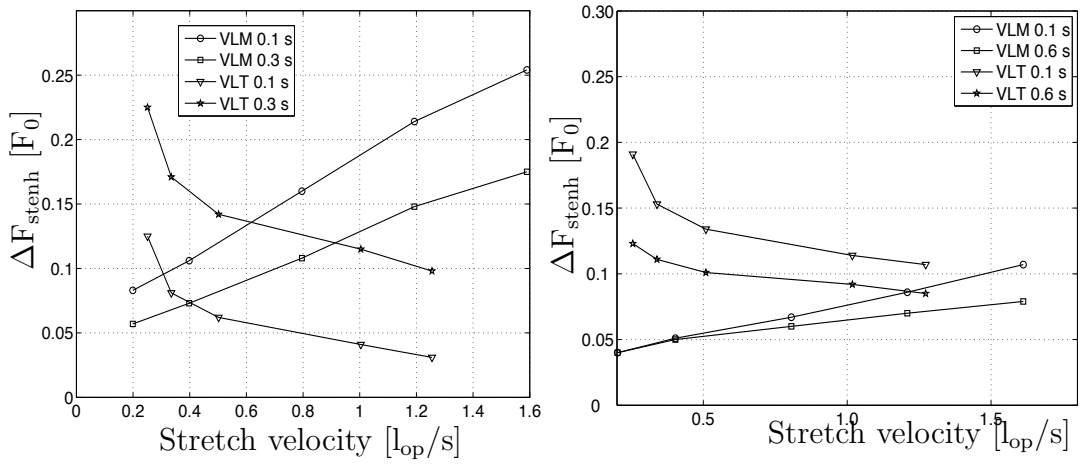

Figure 4.7: Steady-state force enhancement, F_{stenh}, as a function of stretch velocity of EDL (left) and SOL (right) muscles. EDL muscles were pre-activated for $t_0 - t_1 = 0.1$ s or $= 0.3$ s and SOL muscles for $t_0 - t_1 = 0.1$ s or $= 0.6$ s. Average values for group (n = 6).

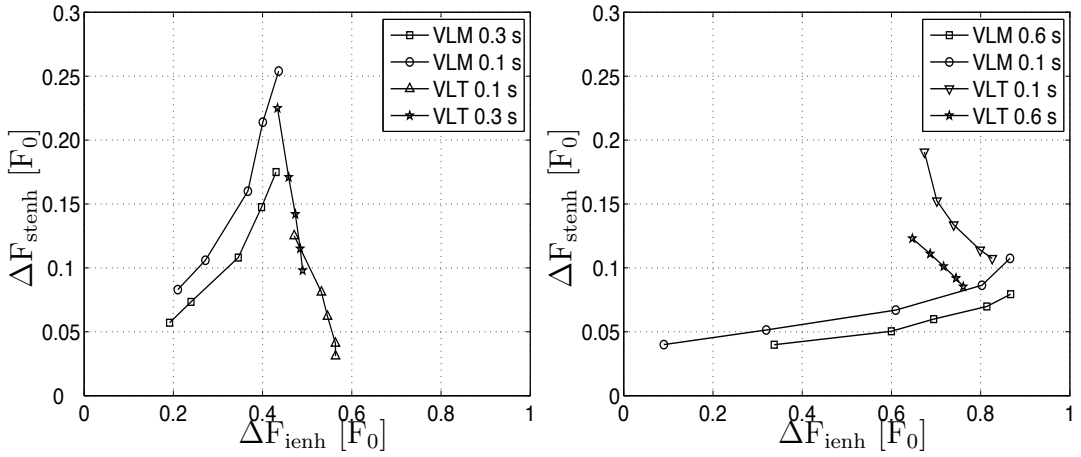

Figure 4.8: Average steady-state force enhancement, $\Delta F^{\mathrm{av}}_{\mathrm{stenh}}$, as a function of instant force enhancement, $\Delta F^{\mathrm{av}}_{\mathrm{ienh}}$ of EDL (left) and SOL (right) muscles. EDL muscle was pre-activated for 0.1 s and 0.3 s and SOL muscle for 0.1 s and 0.6 s.

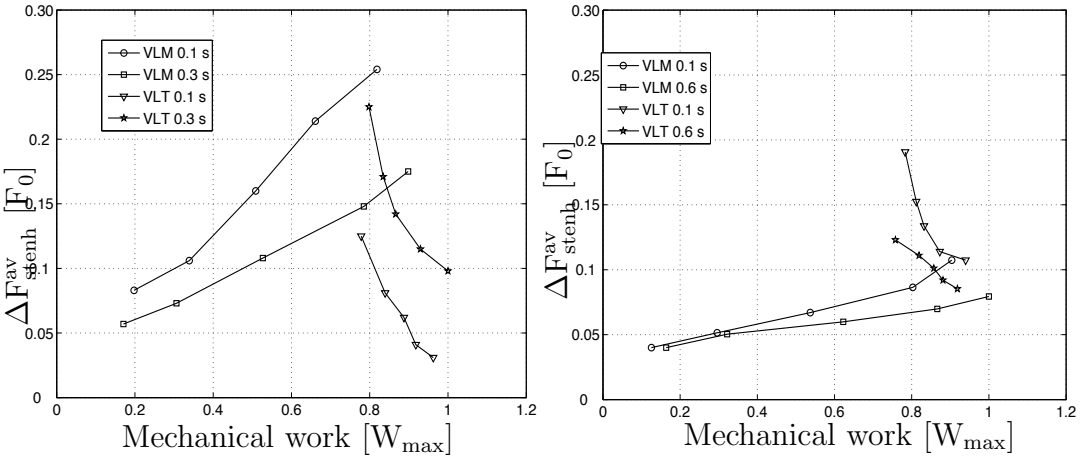

Figure 4.9: Average steady-state force enhancement, $\Delta F^{\mathrm{av}}_{\mathrm{stenh}}$, as a function of mechanical work, W_L, of EDL (left) and SOL (right) EDL muscles were pre-activated for $t_0 - t_1 = 0.1\ s$ or $= 0.3\ s$ and SOL muscles for $t_0 - t_1 = 0.1\ s$ or $= 0.6\ s$.

The experiments also contradicted the statement that the steady-state force enhancement is positively correlated with the instant force enhancement during stretch. Again, the comparison of VLM and VLT experiments shown in Fig. 4.8 indicate that this statement is true only when the stretch velocity is created by variable stretch magnitude.

In the VLM measurement series the steady-state force enhancement is positively correlated with the instant force enhancement, Fig. 4.8. One of the reasons might be due to the recoil energy which increased with increasing the stretch magnitude

and resulted in greater magnitude of decay when the muscle stretch was ceased. In VLT there was no any clear indication of F_{stenh} dependence on F_{ienh}. In many cases of the experimental results of VLT, there was no distinct correlation between F_{ienh} and F_{stenh}.

The steady-state force enhancement may be associated with the amount of mechanical work absorbed by muscle through actin filament deformation during stretch. The results in VLM indicate a positive correlation between the steady-state force enhancement and the magnitude of mechanical work absorbed during active stretch, Fig. 4.9. Large stretches, which are necessary to enhance elastic energy storage and release, cause *contractile element* ('CE') lengthening, i.e., cross-bridge cycling, of which cross-bridge detachment forms a part; during cross-bridge cycling in eccentric movements, mechanical energy is stored in the attached cross-bridges, and this work is lost if these cross-bridges detach, (Ettema et al. 1990).

In VLT steady-state force enhancement was negatively correlated to the magnitude of mechanical work absorbed , Fig. 4.9. In this experimental series there should be no difference in the amount of energy dissipated as heat during relaxation because the stretch magnitude was constant in all VLT tests, and this could not be a reason why the steady-state force enhancement was negatively correlated to the absorbed mechanical work. Meanwhile, there was a difference in stretch time which affected the redistribution of cross-bridges. In shorter stretch duration, there was not enough time for a change of cross-bridges state to occur and all of the change was due to the elasticity. However, energy could also be stored by cross-bridges being dragged into higher energy states during stretch, (Linari et al. 2003). This means that the fast stretched muscle relaxed into lower steady-state force enhancement than the slower stretched muscle due to insufficient duration of stretch to involve all the cross-bridges, including those not attached at the start of the stretch. According to Ettema et al. (1990), for a given active stretch amplitude, a longer active stretch duration (i.e., lower stretch velocity) leads to a stiffer *series elastic component* ('SEC') during the last period of stretch. This means that during such stretches relatively less of the extension of the muscle-tendon complex is taken up by the SEC, causing more CE lengthening and thus energy loss. The higher force enhancement levels are probably caused by a longer activation time during stretch. According to Syme and Grattan (2002), in EDL muscle there was no change in the total work with changes in the velocity of stretch, while in SOL muscle there was a small increase in total work when stretch velocity was increased. Our results show that EDL and SOL muscles behave in similar manner; the work increased very little with increasing stretch velocity, as force during stretch was only to a low degree dependent on velocity. Therefore recoil energy might be one of the mechanisms which contributed to the loss of energy during relaxation, which led to the lower steady-state force enhancement of the faster stretched muscle.

In all experiments, since the stretch took place on the ascending limb, the role of the molecular spring *titin* and passive structural components were not considered. Besides, in all our experimental results (in both VLM and VLT measurement series), there was no observation of passive force enhancement at the end of stimulation which might be generated by titin and passive structural components. Titin is as-

sumed to produce many of the passive forces that come about in most muscles, somewhere in the plateau region and the descending limb of the force-length relationship, (Herzog 1999). Furthermore, it cannot be argued that there is a good evidence that part of steady-state force enhancement originates from a passive structural component, because the passive component only takes effect at long muscle length and is always smaller than the total steady-state force enhancement, (Herzog and Leonard 2002).

With respect to activation time, the steady-state force enhancement, ΔF_{stenh} of EDL and SOL muscles had different properties. In VLM, ΔF_{stenh} of EDL was negatively correlated with pre-activation time, while in VMT, ΔF_{stenh} was positively correlated to pre-activation time. In SOL muscle, ΔF_{stenh} was negatively correlated with pre-activation time in both measurement series, Tables 4.2 – 4.5. One of the reasons might be the consumption of energy during early isometric phase. Pre-activating with $0.1s$, EDL muscle produced almost maximum force, while SOL muscle produced much less than the maximum isometric force before the start of stretch. Pre-activating with 0.3 s on the other hand, EDL produced maximum force, thus consuming more energy which might affect the steady-state force enhancement. In Figs. 4.2 and 4.3, there is an indication that force decreased marginally before the muscle was stretched. There is also a correlation between steady-state force enhancement following stretch and the relaxation time constant, τ_f, of relaxed isometric force. In VLM measurement series, the relaxation time constant of SOL muscle was negatively correlated with the steady-state force enhancement, while in VLT the time constant was positively correlated with the force enhancement, regardless of pre-activation. EDL muscle behaved differently depending on pre-activation. Pre-activating with 0.1 s the relaxation time constant of EDL muscle from both VLM and VLT was negatively correlated with steady state force enhancement. Pre-activating with 0.3 s the relaxation time constant was negatively correlated with steady-state force enhancement in VLM and positively correlated in VLT.

Chapter 5

Conclusions and future work

5.1 Concentric contractions

The performed experiments on mouse EDL and SOL muscles indicate that neither shortening velocity nor force depression during shortening are good predictors for the force depression after concentric contraction. The best predictor for this depression was found to be related to the mechanical work produced by the muscle during active shortening. Mechanical work might not only be a descriptor of steady-state force depression but may point directly to an underlying mechanism. Although the present experimental data is far from complete, there is an indication that the mechanical work affects force depression after shortening. The force depression during an active isometric state following active shortening is affected by the active isometric force reached before the shortening. The force depression is positively correlated to pre-activation. However, for a definite conclusion regarding the role of pre-activation, more data on different pre-activation timings, for instance letting the isometric force reach the maximum before shortening, need to be evaluated. The asymptotic force in the active isometric state following active shortening was in the performed experiments reached through an exponential function with a time constant τ_{r} rather close to the rise time constant for active isometric conditions at optimum length. To draw further conclusions, experiments with longer stimulation times following shortening need to be performed.

5.2 Eccentric contraction

The performed experiments on mouse EDL and SOL muscle indicate that neither stretch velocity nor force enhancement during stretch are good predictors for the force enhancement during isometric contraction immediately following an activated stretch. However, force enhancement was found to be to some extend related to the mechanical work absorbed by the muscle during active stretch, Fig. 4.9. There is an indication of mechanical work dependence of force enhancement, but more studies are needed in order to make a conclusion that mechanical work is predictive for the

mechanisms behind force enhancement. The relaxation time constant is related to the energy lost as heat during muscle relaxation and, consequently, it affects the steady-state force enhancement. Meanwhile, to get more reliable relaxation time constants, the stimulation duration after stretch needs to be longer than in the present study. The force enhancement during an active isometric state following active stretch is affected by the active isometric force reached before the stretch, which is also depending on pre-activation time. To get a clearer picture of the situation, however, the muscles need to be activated with different pre-activation timings so that isometric force reaches a maximum before stretch is initiated.

5.3 Future research

Prediction of muscle forces using mathematical models provides a basis for understanding normal and pathological movement patterns, but these models require quantitative knowledge about their components and parameters. The validity of any model lies not only in its ability to represent observed physiological phenomena, but primarily in its ability to predict accurate results. The muscle model needs to consider structural, physiological, and mechanical properties. The physiological properties relate to fiber-type distribution, fatigue properties, among others. The structural properties relate to fiber arrangement within the muscle and size of the muscle. The mechanical properties are primarily described by the force-length relationship, force-velocity relationship and force-time properties.

Because the experimental protocol consists only of isometric, concentric and eccentric contractions using the methods described in chapter 1.7, we need further measurement using a modified method in order to determine further parameters which describe the property of muscle. From our experiment, the parameters we get are: muscle optimum length (l_{op}) muscle maximum force (F_0), muscle mass (m), maximum shortening velocity ($v_{\max}$). From these parameters we calculated muscle physiological cross sectional area (PCSA). These characteristics are supposed to define the basic properties of the muscle specimens. The performed experiments consisted of prescribed variations of stimulation and length. These, together with the resulting force productions, were used to evaluate some descriptive parameters for the experiments. In addition to force production, and muscle length variation velocity, important data were seen to be the mechanical work done by the muscle during shortening and mechanical work done on the muscle during muscle stretch.

Future work should focus on addressing some mechanical properties that effect muscle force production in different situations:

- *Stiffness and viscoelasticity*: Due to undamped structure within the sarcomeres, such as the cross-bridges, (Huxley 1974), and actin and myosin filaments, (Huxley et al. 1994), muscle responds elastically to very abrupt length change, (Mantovani et al. 1999). The cross-bridge distribution within the sarcomeres on the other hand, are modified by introduction of length changes on the contracting muscle. The passive elasticity between the sarcomeres, may

be recruited by stretching the muscle, (Morgan 1990; Morgan et al. 1996). These factors may affect the elastic properties of muscle and many scientists such as Julian and Morgan (1979); Reich et al. (2000) have investigated the effect. According to Julian and Morgan (1979), the muscle stiffness on the descending limb, remains constant during stretch. Because of its mechanical impedance, it can resist imposed external disturbances. Muscles' spring-like and viscosity properties are extremely important in controlling posture and ensuring stable mechanical behaviors when interacting with the surrounding, (Winters and Crago 2000). The mechanical impedance of muscle varies with activation level. As a consequence, the musculoskeletal system can modify its mechanical properties to adapt according to the demands of specific task, (Winters and Crago 2000). Mutungi and Rantunga (1998) stated that the viscous tension is thought to arise from viscous resistance to stretch between thick and thin filaments in each half sarcomere, whereas the viscoelasticity and elasticity may result from other structural elements such as the gap filament and the cytoskeleton. Quick-release experiments may be interpreted to provide direct evidence of the existence of a series elastic component, (McMahon 1984)

- *Residual force enhancement*: Edman et al. (1978, 1982) were the first to propose that the residual force enhancement after stretch was compatible with recruitment of a passive elastic element in parallel with the contractile system. This notion was further supported by indirect evidence in single fiber and whole muscle preparations, (Lee and Herzog 2002) and was used in theoretical considerations, (Herzog 1998; Herzog and Leonard 2002). Herzog (2001) proposed that force enhancement following muscle stretch is composed of two components: an active and a passive force enhancement. The active component is associated with an increase in the number of attached cross-bridges and the passive component is associated with the molecular spring *titin*. To investigate the existence of this passive force enhancement, the active stretch (eccentric contraction) should be performed on both the ascending and descending limbs of force-length relationship of muscle. The eccentric contractions should be carried out, below, above and through the optimum length. This experiment should be performed with different stretch magnitudes over different stretching times. The stimulation time should be longer after the end of the stretch so that the muscle relaxes completely to the steady-state level. If any difference is observed, then there might be a contribution of this mechanical property to the steady-force enhancement following active muscle stretch. From our experimental results, no passive force enhancement was observed. All the stretches were done on the ascending limb of force-length relationship where there is no passive force.

- *Recoil energy*: A contracting muscle resists stretching with a force greater than it can exert at a constant length. If the muscle is kept active at the stretched length, the excess tension decays exponentially to the steady-state enhanced level. The recoil elastic energy is proportional to the amount of energy stored, and can be studied using a stretch-shortening cycle method. This leads to a

greater work output than in a simple shortening contraction. Measurements on work done during shortening, work needed to the stretch muscle and work done during shortening following muscle stretch could be useful. From this, according to (Syme and Grattan 2002), the net energy gain or loss can be calculated using the relation,

$$E_{rec} = \frac{W_{st-sh} - W_{sh}}{W_{st}} \tag{5.1}$$

where E_{rec} energy recovery; W_{st-sh} work done during shortening following muscle stretch; W_{sh} work done during shortening; and W_{st} work needed to stretch muscle. The test can be performed in different transient periods between stretch and shortening and would show if the muscles can demonstrate different amount of storage of elastic energy. If there is any difference, it can be interpreted through differences in sarcomere crossbridge life times between fast and slow muscle fibers. The slow type muscle may be able to retain the cross-bridge attachment for a longer period of time and therefore it may utilize elastic energy better in a slow type of motion.

Bibliography

T. Allinger, W. Herzog, and M. Epstein. Stability of muscle fibers on the descending limb of the force-length relation: A theoretical consideration. *J. Biomech.*, 29: 627–633, 1996.

M. Bagni, G. Cecchi, B. Colombini, and F. Colomo. A non-cross-bridge stiffness in activated frog muscle fibers. *Biophys J*, 82:3118–3127, 2002.

K. S. Campbell and M. Lakie. A cross-bridge mechanism can explain the thixotropic short-range elastic component of relaxed skeletal muscle. *J. Physiol.*, 510.3:941–962, 1998.

G. A. Cavagna, M. Mazzant, N. C. Heglund, and G. Citterio. Storage and release of mechanical energy by active muscle: A non-elastic mechanism. *J. Exp. Biol.*, 115:79–87, 1985.

D. B. Chaffin and G. J. Andersson. *Occupational biomechanics*. Wiley, New York, 1991.

K. A. P. Edman, C. Caputo, and F. Lou. Depression of tetanic force induced by loaded shortening of frog muscle fibers. *J. Physiol.*, 466:535–552, 1993.

K. A. P. Edman, G. Elzinga, and I. M. Noble. Enhancement of mechanical performance by stretch during tetanic contractions of vertebrate skeletal muscle fibers. *J. Physiol.*, 281:139–155, 1978.

K. A. P. Edman, G. Elzinga, and I. M. Noble. Residual force enhancement after stretch of contracting frog single muscle fibers. *J. Physiol.*, 80:769–784, 1982.

G. J. C. Ettema, P. A. Huijing, G. J. van Ingen Schenau, and A. de Haan. Effects of prestretch at the onset of stimulation on mechanical work output of rat medial gastrocnemius muscle-tendon complex. *J. Exp. Biol.*, 152:333–351, 1990.

G. J. C. Ettema and K. Meijer. Muscle contraction history: modified Hill versus an exponential decay model. *Biol. Cybern.*, 83:491–500, 2000.

D. Fredrick. Making the most of muscle. There's more to muscle than fast-twitch and slow-twitch. *Velo News*, 33/no. 19, 2004.

Y. C. Fung. *Biomechanics, Mechanical properties of living tissues*. Springer, New York, 1993.

H. Gissel and T. Clausen. Excitation-induced Ca^{2+} influx in rat soleus and edl muscle: mechanisms and effects on cellular integrity. *Am. J. Physiol. Regulatory Integritive Comp. Physiol.*, 279:R917–R924, 2000.

A. M. Gordon, E. Homsher, and M. Regnier. Regulation of contraction in skeletal muscle. *Physiol. Rev.*, 80:853–924, 2000.

J. E. Gregory, D. L. Morgan, and U. Proske. Tendon organs as monitors of muscle damage from eccentric contractions. *Exp. Brain Research*, 151:346–355, 2003.

W. Herzog. History dependence of force production in skeletal muscle: a proposal for mechanism. *J. Electromyog. Kinesiol.*, 8:111–117, 1998.

W. Herzog. *Skeletal Muscle Mechanics, From Mechanics to Function*. Wiley, Calgary, 1999.

W. Herzog. The nature of force depression and force enhancement in skeletal muscle contraction. *Eur. J. Sport Sci.*, 1:1–14, 2001.

W. Herzog and T. R. Leonard. Depression of cat soleus force following isokinetic shortening. *J. Biomech.*, 30:865–872, 1997.

W. Herzog and T. R. Leonard. The history dependence of force production in mammalian skeletal muscle following stretch-shortening and shortening-stretch cycles. *J. Biomech.*, 33:531–542, 2000.

W. Herzog and T. R. Leonard. Force enhancement following stretching of skeletal muscle: a new mechanism. *J. Exp. Biol.*, 205:1275–1283, 2002.

W. Herzog and T. R. Leonard. The role of passive structure in force enhancement of skeletal muscles following stretch. *J. Biomech.*, 38:409–415, 2005.

W. Herzog, T. R. Leonard, and J. Z. Wu. Force depression following skeletal muscle shortening is long lasting. *J. Biomech.*, 31:1163–1168, 1998.

W. Herzog, T. R. Leonard, and J. Z. Wu. The relationship between force depression following shortening and mechanical work in skeletal muscle. *J. Biomech.*, 33: 659–668, 2000.

W. Herzog, R. Schachar, and T. R. Leonard. Characterization of the passive component of force enhancement following active stretch of skeletal muscle. *J. Exp. Biol.*, 206:3635–3643, 2003.

A. Hill. The heat of shortening and the dynamic constants of muscle. *Proc. Royal Soc. London*, B 126:136–195, 1938.

A. Hill. *First and last experiments in muscle mechanics*. Cambridge University Press, Cambridge, U.K, 1970.

A. F. Huxley. Muscular contraction. *J. Physiol.*, 243:1–43, 1974.

A. F. Huxley, A. Steward, H. Sosa, and T. Irving. X-ray diffraction measurements of the extensibilty of actin and myosin filaments in contracting muscle. *J. Biophys.*, 67:2411–2421, 1994.

R. S. James, I. S. Young, V. M. Cox, D. F. Goldspink, and J. D. Altringham. Isometric and isotonic muscle properties as determinants of work loop power output. *Eur. J. Physiol.*, 432:767–774, 1996.

C. Johansson, P. K. Lunde, S. Göthe, J. Lännergren, and H. Westerblad. Isometric force and endurance in skeletal muscle of mice devoid of all known thyroid hormone receptors. *J. Physiol.*, 547.3:789–796, 2003.

R. K. Josephson and D. R. Stokes. Work-dependent deactivation of a crustacean muscle. *J. Exp. Biol.*, 202:2551 – 2565, 1999.

F. J. Julian and D. L. Morgan. The effect on tension of nonuniform distribution of length change applied to frog muscle fibers. *J. Physiol.*, 293:379–392, 1979.

A. M. King, D. S. Loiselle, and P. Kohl. Force generation for locomotion of vertebrates: Skeletal muscle overview. *IEEE J. Oceanic Eng.*, 29, 2004.

P. Lagreneur, B. Morlon, and J. Van Hoecke. Simulation of in situ soleus isometric force output as a function of neural excitation. *J. Biomech*, 29.11:1455–1462, 1996.

H. Lee and W. Herzog. Force enhancement following muscle stretch of electrically and voluntarily activated human adductor pollicis. *J. Physiol.*, 545:321–330, 2002.

H. Lee and W. Herzog. Force depression following muscle shortening of voluntarily activated and electrically stimulated human adductor pollicis. *J. Physiol.*, 551: 993–1003, 2003.

T. R. Leonard and W. Herzog. Does the speed of shortening affect steady-state force depression in cat soleus muscle? *J Biomech*, 38:2190–2197, 2004.

R. L. Lieber and J. Fridén. Functional and clinical significance of skeletal muscle architecture. *Muscle Nerve*, 23:11:1647–1666, 2000.

M. Linari, R. C. Woledge, and N. A. Curtin. Energy storage during stretch of active single fibres from frog skeletal muscle. *J. Physiol*, 548:461–474, 2003.

S. L. Lindstedt, P. C. LaStayo, and T. E. Reich. When active muscles lengthen: Properties and consequences of eccentric contractions. *News Physiol. Sci.*, 16: 256–261, 2001.

R. Lovering, M. Hakim, C. Moorman, and P. De Dyne. The contribution of contractile pre-activation to loss of function after a single lengthening contraction. *J. Biomech.*, 38:1501–1507, 2005.

M. Mantovani, G. A. Cavagna, and N. C. Heglund. Effect of stretching on undamped elasticity in muscle fibres from rana temporaria. *J. Muscle Research and Cell Motility*, 20:33–43, 1999.

G. Maréchal and L. Plaghki. The deficit of the isometric tetanic tension redeveloped after release of frog muscle at a constant velocity. *J. Gen. Physiol.*, 73:453–467, 1979.

T. A. McMahon. *Muscles, Reflexes, and Locomotion*. Princeton University Press, Princeton, New Jersey, 1984.

D. L. Morgan. New insight into the behavior of muscle during active lengthening. *Biophys. J.*, 57:209–221, 1990.

D. L. Morgan. An explanation for residual increased tension in striated muscle after stretch during contraction. *Exp. Physiol.*, 79:831–838, 1994.

D. L. Morgan, D. R. Claflin, and F. J. Julian. The effect of repeated active stretches on tension generation and myoplasmic calcium in frog single muscle fibres. *J. Physiol.*, 497:665–674, 1996.

D. L. Morgan, N. Whithead, A. Wise, J. Gregory, and U. Proske. Tension changes in the cat soleus muscle following slow stretch or shortening of the contracting muscle. *J. Physiol.*, 522.3:503–513, 2000.

G. Mutungi and K. W. Rantunga. Temperature-dependent changes in the viscoelasticity of intact resting mammalian (rat) fast- and slow-twitch muscle. *J. Physiol.*, 508.1:253–265, 1998.

B. N. Nigg and W. Herzog. *Biomechanics of the musculo-skeletal system*. 2nd ed. Wiley, New York, 1999.

N. Palastanga, D. Field, and R. Soames. *Anatomy and human movement*. Butterworth Heinemann, Oxford, 2002.

U. Proske, J. E. Gregory, D. L. Morgan, P. Percival, N. S. Weerakkody, and B. J. Canny. Force matching errors following eccentric exercise. *Human Movement Sci.*, 23:365 – 378, 2004.

D. E. Rassier and W. Herzog. Considerations on the history dependence of muscle contraction. *J. Appl. Physiol.*, 96:419–427, 2004.

D. E. Rassier, W. Herzog, and D. Syme. Stretch-induced, steady-state force enhancement in single skeletal muscle fibers exceeds the isometric force at optimum fiber length. *J. Biomech.*, 36:1309 – 1316, 2003.

D. E. Rassier, B. R. MacIntosh, and W. Herzog. Length dependence of active force production in skeletal muscle. *J. Appl. Physiol.*, 86:1445–1457, 1999.

T. E. Reich, S. L. Lindstedt, P. C. LaStayo, and D. J. Pierotti. Is the spring quality of muscle plastic? *Am. J. Physiol.*, 278:1661–1666, 2000.

B. Roszek, G. Baan, and P. Huijing. Decreasing stimulation frequency-dependent length-force characteristics of rat muscle. *J. Appl. Physiol.*, 77:2115–2124, 1994.

T. G. Sandercock and C. J. Heckman. Force from cat soleus muscle during imposed locomotor-like movement: experimental data versus Hill-type model prediction. *Amer. Physiol. Soc.*, 1997.

D. A. Smith and M. A. Geeves. Strain-dependent cross-bridge for muscle. *Biophys. J.*, 69:524–537, 1995.

A. Stuart, S. K. Lee, A. P. Fritz, and L. Kucharski. New look at force-frequency relationship of human skeletal muscle: Effects of fatigue. *J. Neurophysiol.*, 79: 1858–1868, 1998.

H. Sugi and T. Tsuchiya. Stiffness changes during enhancement and deficit of isometric force by slow length changes in frog skeletal muscle. *J. Physiol.*, 407:215–229, 1988.

D. A. Syme and M. J. Grattan. Effects of stretch on work from fast and slow muscles of mice: damped and undamped energy release. *Can. J. Physiol. Pharmacol.*, 80: 887–900, 2002.

A. J. van den Bogert, K. G. M. Gerritsen, and G. K. Cole. Human muscle modelling from a user's perspective. *J. Electromyogr. Kinesiol.*, 8:119–124, 1998.

D. A. Winter. *Biomechanics and motor control of human movement*. Wiley, Ontario, 2005.

J. M. Winters and P. E. Crago. *Biomechanics and neural control of posture and movement*. Springer, New York, 2000.

F. Zajac. Muscle and tendon: Properties, models, scaling and application to biomechanics and motor control. *Crit. Rev. Biomed. Eng.*, 17:359–411, 1989.

C. J. Zuubier, M. B. Lee-de Groot, W. J. Van der Laarse, and P. A. Huijing. Effects of in vivo-like activation frequency on the length-dependence force generation of skeletal muscle fibre bundles. *Eur. J. Appl. Physiol. Occup. Physiol.*, 77:503–510, 1998.